Instrument Science Report STIS 2012-03

Summary of the STIS Cycle 17 Calibration Program

Michael A. Wolfe[1], Rachel A. Osten[1], Svea Hernandez[1], Alessandra Aloisi[1], Ralph Bohlin[1], K. Azalee Bostroem[1], Rosa Diaz[1], Van Dixon[1], Justin Ely[1], Phil Hodge[1], Danny Lennon[1], Elena Mason[1], Sami-Matias Niemi[1], Illaria Pascucci[4], Charles Proffitt[2], Tom Wheeler[1], and Wei Zheng[3]

[1]Space Telescope Science Institute, Baltimore, MD
[2]Space Telescope Science Institute/Computer Sciences Corporation, Baltimore, MD
[3]Johns Hopkins University, Baltimore, MD
[4]University of Arizona, Tucson, AZ

May 8, 2013

ABSTRACT

We summarize the status of the calibration program for the Space Telescope Imaging Spectrograph during Cycle 17, which ran from August 2009 until October 2010.

- Introduction (page 2)
- Overview of Calibration and Monitoring Programs (page 3)
- CCD Monitoring and Detector Calibration (page 5)
- MAMA Monitoring and Detector Calibration (page 31)
- Operations, Engineering, and Special (page 44)
- Supplemental Calibrations (page 55)
- Appendix (page 62)

Operated by the Association of Universities for Research in Astronomy, Inc., for the National Aeronautics and Space Administration.

1. Introduction

The Space Telescope Imaging Spectrograph (STIS) was successfully repaired during Servicing Mission 4 (SM4) in May 2009 and allowing it to resume science observations. With the instrument fully restored the STIS team continued to perform monitoring, supplemental and special calibration programs. The calibration plan is mainly based on optimized and improved monitoring and calibration programs executed in previous cycles. Cycle 17 was the seventh cycle in which STIS was employed in producing scientific observations.

The STIS Cycle 17 calibration and special monitoring programs executed from August 2009 through October 2010. The 15-month duration of these programs overlapped with SMOV4, Cycle 17, and Cycle 18 science observations. At the start of the Cycle 17 calibration program the number of external orbits allocated was 53 and the number of internal plus parallel orbits was 2172. Halfway through Cycle 17, supplemental calibration programs were designed to expand upon on-orbit operations during SMOV4 and early Cycle 17 observations (both internal and external). The supplemental programs included 4 external orbits and 15 internal plus parallel orbits. The orbit allocation and execution of Cycle 17 calibration and supplemental programs are summarized in Table 1.

Table 1. Summary of orbit allocation and execution during Cycle 17 for STIS calibration and supplemental programs.

	External		Internal + Parallel	
	Regular	Supplemental	Regular	Supplemental
Allocated	66	4	2179	15
Executed	71	4	1773	15
Withdrawn	3	0	410	0
Failed	8	0	25	0
Repeated	8	0	4	0

Internal orbit visits are normally limited to a total of 1800 seconds so that the exposures can be taken during occultations of external targets. If calibration visits require more than 1800 seconds then these calibration visits are taken in pure parallel mode. The CCD Hot Pixel Annealing Program (11849, 204 orbits), the CCD Internal Sparse Field Test (11850, 74 orbits), and the MAMA FUV and NUV Flat Program (11861 and 11862, 14 and 11 orbits, respectively) required more than 1800 second orbits.

The monitoring programs in Cycle 17 are essentially reproductions of monitoring programs from previous cycles. These programs assess stability of the CCD, provide information on the dark current, bias level, read out noise, spurious charge, charge transfer efficiency (CTE), growth of hot pixels, slit wheel repeatability, CCD and MAMA dispersion solutions, MAMA focus monitor, MAMA fold distribution, and sensitivity monitoring for both the CCD and MAMA detectors. The Cycle 17 supplemental

programs provided additional exposures for the MAMA FUV Flats, the MAMA Dark Monitoring, MAMA spectroscopic sensitivity and data for the verification of adjustment to two STIS MSM positions and determination of the STIS PtCr/Ne lamp ratios.

The ultimate goal of the Cycle 17 special calibration programs is to produce reference files used in the calibration of STIS data. Currently available reference files can be found at:
www.stsci.edu/hst/observatory/cdbs/SIfileInfo/STIS/reftablequeryindex. Other products generated from the calibration programs include STIS Instrument Science Reports (ISRs), STIS Technical Instrument Reports (TIRs), updates to the STIS Instrument (IHB) and Data (DHB) Handbooks. Links to the aforementioned documents can be found at:
www.stsci.edu/hst/stis/documents. Note that the TIRs are normally intended for internal STScI use. In order to retrieve TIRs a document request needs to be sent to **help@stsci.edu**. The information derived from the monitoring and calibration proposals contributed to numerous papers written in regards to the 2010 HST Calibration Workshop (Deustua and Oliveira 2010). These papers are listed in the Appendix along with other external and internal publications as well as delivered reference files.

2. Overview of Calibration and Monitoring Programs

Summaries of each Cycle 17 monitoring and calibration program can be found in Table 2. The first two columns present the Proposal ID and its title (note that the Bias and Dark Monitors are counted as one program). Columns 3 and 4 contain the number of external and internal orbits (executed and allocated, with the latter reported in square brackets). Column 5 and 6 detail the products delivered and the accuracy achieved, respectively. The last column of Table 2 presents the ISR page on which detailed information for that program can be found.

The following sections provide detailed information on the purpose, execution, summary of analysis and accuracy achieved for the individual calibration proposals in the Cycle 17 program.

Table 2. Summary of Cycle 17 calibration and monitoring programs. Further details can be found in the following sections.

ID	Proposal Title	Time Used (orbits) executed [allocated]		Products	Accuracy Achieved	Page
		External	Internal			
CCD Monitoring and Detector Calibration						
11843	CCD Performance Monitor		24[27]	CCD Reference File	> 0.1 ADUs	5
11844 & 11845	CCD Dark Monitor		906[976]	Reference Files	S/N $\approx$ 1.15	9
11846 & 11847	CCD Bias Monitor		454[488]	Reference Files	S/N $\approx$ 1.0 and greater	12
11848	CCD Read Noise Monitor		18[20]	Web Page Updates	0.14 ADUs (gain = 1) and 0.032 ADUs (gain = 4)	14
11849	CCD Annealing Monitor		85P[204P][a]	Web Page Updates	average growth rate is 3.67% per month	17
11850	CCD Charge Transfer Efficiency Monitor		74P[74P][a]	CCD Reference File	1% for signal > 200 e-	19
11852	CCD Spectroscopic Flats		50[50]	PFL Reference File, TIR	$< 1\%$ residual scatter	23
11853	CCD Imaging Flats		12[12]	PFL Reference File	$> 0.5\%$ residual scatter	24
11854	CCD Full-Field Sensitivity	1[1]		ISR, STAN if needed	$< 1\%$ change in PHOTFLAM values	25
11855	CCD Spectroscopic Sensitivity	10[10]		TDS Reference File	S/N of 50 at wavelength of least sensitivity	26
11858	CCD Dispersion Solution		7[7]	Updated Dispersion Solution	zero-points 0.1 pixels; relative 0.2 pixels	30
MAMA Monitoring and Detector Calibration						
11856	MAMA Full-Field Sensitivity	3[3]		ISR, STAN if needed	variations across detector $< 5\%$	31
11857	MAMA Dark Monitor		106[288]	Dark reference image for shape, TDC file for time dependence, ISR	dark subtraction (NUV) < 0.0005 cnts/s/pix	32
11859	MAMA Dispersion Solution		10[10 + 3P][a]	Updated Dispersion Solution	zero-points 0.1 pixels; relative 0.2 pixels	34
11860	MAMA Spectroscopic Sensitivity and Focus Monitor	14[16]		TDS Reference File, Update Focus (Data not analyzed)	S/N > 50 for G140L, G230L S/N (E and M modes) at $\lambda_{\rm cen}$ 35 - 40	35
11861	MAMA FUV Flats		16[14]	PFL Reference File	$> 1.0\%$ residual scatter high res	38
11862	MAMA NUV Flats		13[11]	PFL Reference File	$> 1.0\%$ residual scatter high res	40
11866	MAMA Echelle Blaze Function Zero Points	29[24]		PHT Reference File ISR/TIR	accuracy of sensitivity curves $< 0.1\%$	42
Operations, Engineering, and Special						
11851	CCD Slit Wheel Repeatability		1P[1P][a]	STAN	≈ 0.2 pixels	44
11863	MAMA Fold Distribution		4[4]	Report	FUV dark current nominal NUV dark current initially high but decreasing with time	45
11864	MAMA Anomalous Recovery	Withdrawn			N/A	50
11865	COS Flux Standard	2[2]			$\sim 1\%$	51
11652	CCD Throughput Calibration of the 52X0.2E1 Aperture	1[1]		GO calibration program	N/A	52
11999	JWST Calibration	15[13]		ISR	flux calibration 1% but not yet achieved	53
Supplemental Calibrations[b]						
12078	Verification of Adjustment of Two STIS MSM Positions		1[1]		G750M c6094 < 1 pixel offset, G430M c5216 5.7 pixel offset, G430M c3305 7.9 pixel offset	55
12079	STIS PtCr/Ne Lamp Ratios		7[7]	ISR	HITM1 flux $> 1.5\times$LINE flux, HITM2 flux $> 3.0\times$LINE flux, HITM2 flux $> 1.5\times$HITM1 flux	60

[a] P refers to pure parallel orbits.

[b] The supplemental programs 11857, 11860, and 11861 have been incorporated into their original programs. Please see these programs in the table.

3. CCD Monitoring and Detector Calibration

Proposal ID 11843: CCD Performance Monitor Program

Purpose and Description of Program

This activity measures the baseline performance and commandability of the CCD subsystem. Bias and flat field exposures are taken in order to measure read noise, gain, spurious charge and charge transfer efficiency (CTE) from the extended pixel edge response test (EPER). CCD performance measurements can be used to update the ccd parameters reference file if needed.

Execution

The execution of the program was nominal. Observations were taken every 6 months and consisted of 8 orbits. No changes were made to the program.

Summary of Analysis

The Read Out Noise (RON) and Gain have remained constant throughout Cycle 17 as reported in Table 3 and 4. The Cycle 17 RON measurements are consistent with SMOV4 results. The spurious charge showed an initial increase in March 2010 but in September 2010 the spurious charge decreased, as shown in Table 5. This behavior is seen with gain settings 1 and 4. The charge transfer inefficiency (CTI) as measured with the EPER test (note that this is a relative measure of CTI, not an absolute one) shows a slight increase in parallel CTI and a sharp increase in serial CTI when compared to SMOV4 results as exhibited in Table 6. Additionally, a temperature dependence can be seen in Figure 1 for the parallel CTI. Statistics of sub-arrays used for target acquisitions show no change for Cycle 17 and have the same results derived during SMOV4 (see Table 8). Additional details can also be found in Proffitt et al. (2010) and Wolfe et al. (2010).

Accuracy Achieved

Read noise error for all binning and gains is greater that 0.1 e- or ADUs. This is greater than the accuracy stated in the Phase I.

Continuation Plans

This program has been continued in Cycle 18 as program 12396.

Table 3. Gain and Read Noise (March 2010 data)

CCD Gain	Binning	Gain (e-)	RON (e-)	Flux (e-, maximum intensity)
1	1x1	1.01 ±0.01	5.64 ±0.10	17393.0
1	1x1	1.00 ±0.01	5.61±0.10	5674.0
1	1x2	1.01±0.02	5.77±0.13	11570.0
1	2x1	1.02±0.01	5.51±0.14	11550.0
1	2x2	0.98±0.02	5.59±0.38	22333.0
2	1x1	2.03±0.03	6.86±0.18	53628.0
4	1x1	4.07±0.03	7.86±0.21	72670.0
8	1x1	8.11±0.06	12.07±0.39	72398.0

Table 4. Gain and Read Noise (September 2010 data)

CCD Gain	Binning	Gain (e-)	RON (e-)	Flux (e-, maximum intensity)
1	1x1	1.00±0.01	5.79 ±0.11	18704.0
1	1x1	1.03±0.01	5.93±0.12	7223.0
1	1x2	1.03±0.01	5.94±0.19	13150.0
1	2x1	1.01±0.01	5.31±0.10	12569.0
1	2x2	1.01±0.02	5.90±0.37	24007.0
2	1x1	2.00±0.02	6.73±0.16	56293.0
4	1x1	4.08±0.04	8.24±0.19	78744.0
8	1x1	8.14±0.03	11.81±0.19	84491.0

Table 5. Spurious Charge

Date	Gain	CCD Position	Spurious Charge (e-)
March 2010	1	Row 512	1.300±0.682
March 2010	1	Row 900	0.819±0.607
March 2010	4	Row 512	6.750±1.420
March 2010	4	Row 900	6.300±1.290
September 2010	1	Row 512	1.210±0.638
September 2010	1	Row 900	0.771±0.499
September 2010	4	Row 512	6.550±1.360
September 2010	4	Row 900	6.140±1.250

Table 6. EPER CTI (12000 e- signal level)

Date	Parallel CTI	Parallel CTI Error	Serial CTI	Serial CTI Error
SMOV4 August 2009	0.00009122	0.00000162	0.00000599	0.00000009
September 2009	0.00008766	0.00000159	0.00000631	0.00000009
March 2010	0.00009237	0.00000166	0.00000665	0.00000010
September 2010	0.00009292	0.00000173	0.00000782	0.00000011

Table 7. Sub-Arrays for Target Acquisitions

Date	Sub-Array Size	Mean (e-)	Stddev (e-)	Median (e-)	S/N
March 2010	100x100	0.2014	0.6769	0.1247	0.298
March 2010	1024x32	0.2339	0.7088	0.2065	0.330
September 2010	100x100	0.2012	0.6767	0.1235	0.297
September 2010	1024x32	0.2339	0.7088	0.2067	0.330

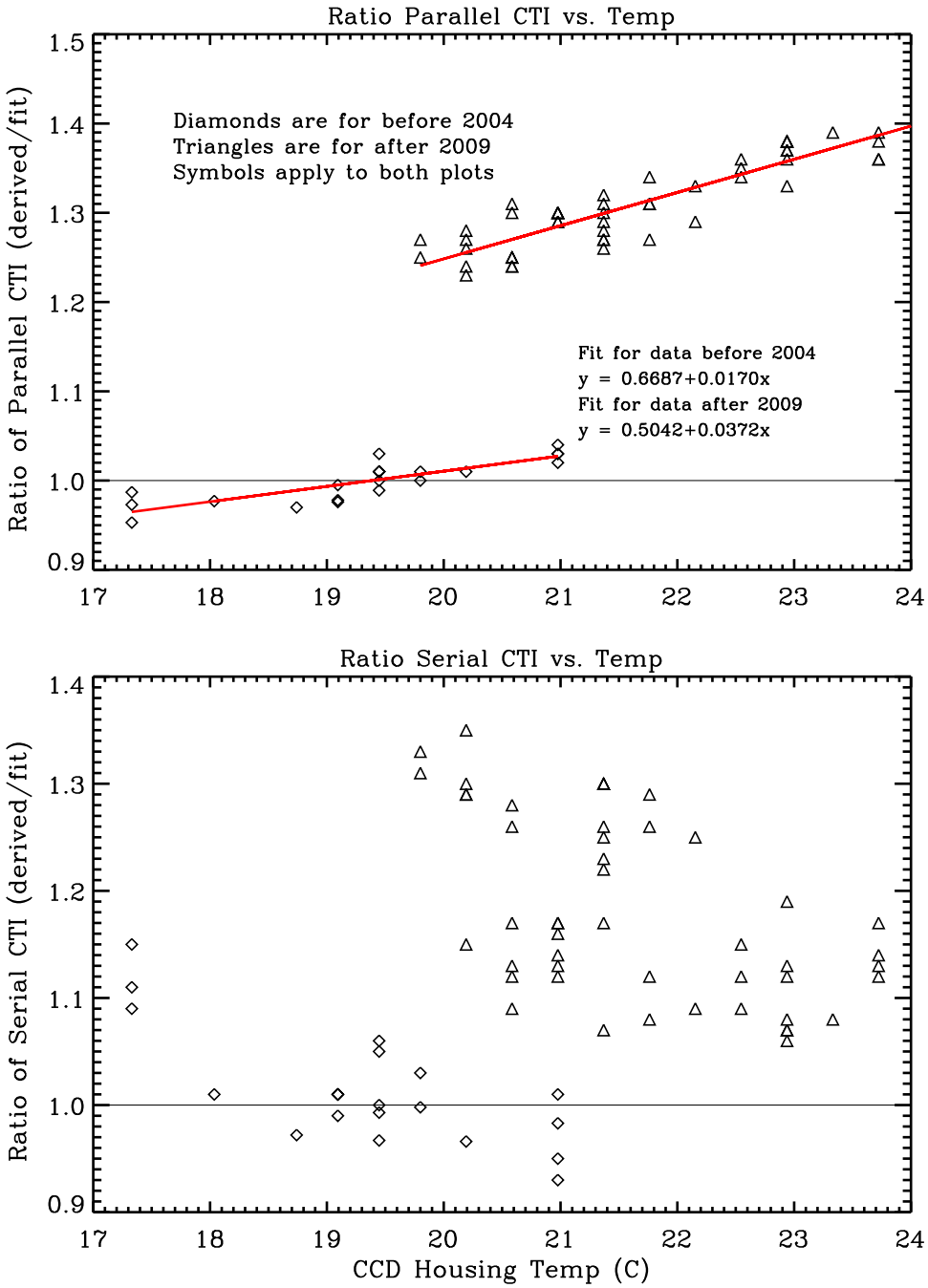

Figure 1. Relationship between the ratio of the derived (measured) values to linear fit values against the CCD housing temperature. Measurements for data taken before SM4 are shown in diamonds. Data taken after SM4 are displayed in triangles. The top plot shows a temperature dependence for the parallel CTI with increasing CTI at higher temperatures. In contrast to the parallel CTI, the serial CTI does not exhibit this temperature dependence (bottom plot).

Proposal ID 11844 & 11845 : CCD Dark Monitor Program

Purpose and Description of Program	The goal was to produce weekly dark reference files from a series of long dark exposures (1100 s). Several short dark exposures (60 s) were taken daily for observers to use to update the hot pixel intensities in the weekly dark reference files using the stsdas script daydarkT.cl.
Execution	906 out of 976 visits were executed. 70 were withdrawn due to scheduling considerations and 14 visits lost all data due to SIC&DH failures. These statistics cover both Cycle 17 calibration proposals.
Summary of Analysis	Data taken between monthly anneals is combined to produce a baseline dark image. Weekly reference dark files are made by using weekly data and used to update the hot pixels in the baseline dark image. The bias reference image for the corresponding time range (between anneals) is used to remove the bias from the dark reference frame. The scatter in dark current appears to have increased in data taken after SM4 when compared to previous calibration cycles before the STIS failure in 2004. Investigation is underway to determine the cause of the scatter and to determine if there are any calibration procedures that can mitigate the dark current scatter. Figure 2 demonstrates that the peak of the distributions of the dark current slightly increased over Cycle 17. Figure 3 shows the median dark rate calculated over the whole CCD as a function of time. Note the increased scatter in the dark rate when compared to previous calibration cycles.
Accuracy Achieved	The dark current ranged from 0.0110 to 0.0120 e-/s/pixel and the S/N is $\approx$ 1.15. There is an ongoing investigation into the scatter inherent in the dark current. Therefore, at this time, it is difficult to calculate a robust accuracy for the dark current.
Continuation Plans	These two programs have been continued in Cycle 18 as programs 12400 and 12401.

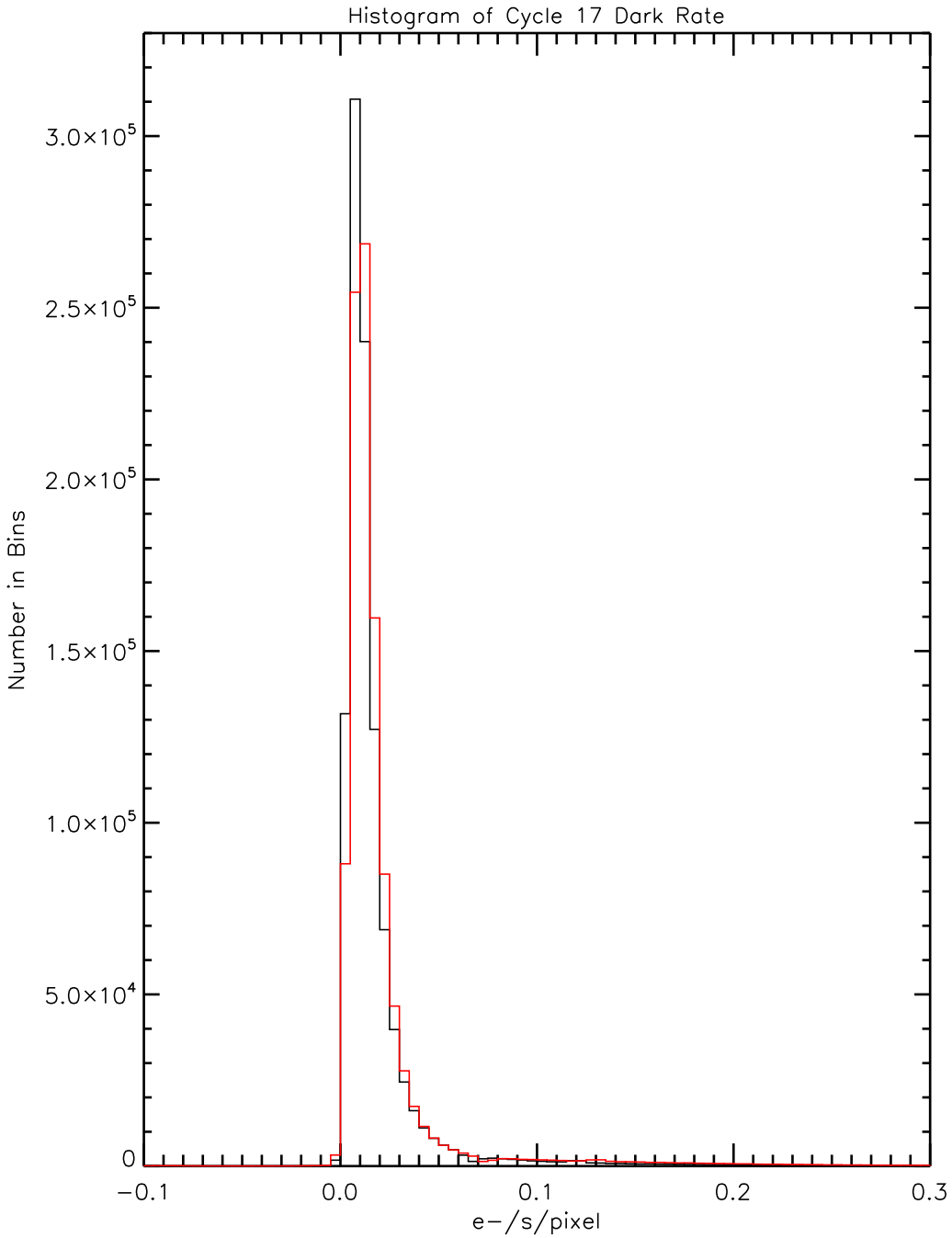

Figure 2. The black histogram is from a dark taken at the beginning of Cycle 17 and the red histogram is of a dark taken at the end of Cycle 17 calibrations. The time span is from August 3, 2009 to October 31, 2010.

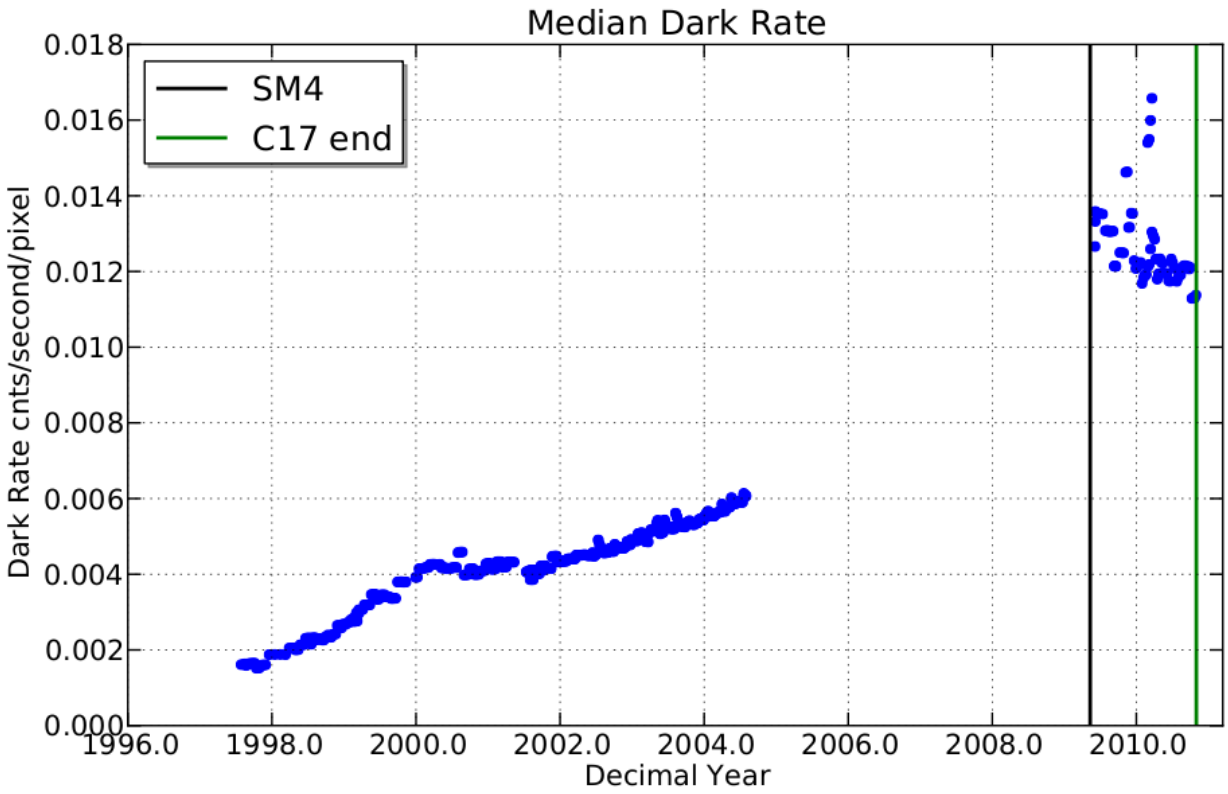

Figure 3. Plot of the median dark rate over the whole CCD as a function of time. Cycle 17 median dark rates can be found between the black vertical solid line (SM4) and the green vertical line (End of Cycle 17). Note the increased scatter in the median dark rates when compared to pre-SM4 values.

Proposal ID 11846 & 11847 : CCD Bias Monitor Program

Purpose and Description of Program	The goal was to produce bias reference files for gain 1 un-binned (weekly files), gain 1 binned 1x2, 2x1, 2x2 (biweekly files) and gain 4 un-binned (biweekly files) with an adequate signal-to-noise to measure hot columns on these time scales.
Execution	454 out of 488 visits were executed. 34 were withdrawn due to scheduling considerations and 7 lost all data due to SIC&DH failures. These statistics cover both Cycle 17 calibration proposals.
Summary of Analysis	Data taken between monthly anneals is combined weekly (gain 1 un-binned) or biweekly (gain 1 binned and gain 4 un-binned) to produce bias reference files. If a weekly or biweekly time period is short of data, the data from that time period are used to update hot columns in a baseline bias image, made from all data taken during that anneal period. This combination thus provides good signal-to-noise in normal columns while updating hot columns.
Accuracy Achieved	This program was designed to achieve a signal-to-noise of at least 1 for each bias reference file. The achieved S/N is given in Table 9 for data taken from August 2009 to October 2010. Note that all S/N measurements are ≈ 1.00 or greater.
Continuation Plans	These two programs have been continued in Cycle 18 calibrations as programs 12402 and 12403.

Table 8. Reference File: Standard Deviation and Signal-to-Noise

Gain	Binning	Number of Exposures	Standard Deviation	Median S/N
1	1x1	98	0.90	1.18
		98	0.90	1.18
1	1x2	28	1.44	1.05
		28	1.35	0.98
1	2x1	28	1.46	1.24
		28	1.39	1.16
1	2x2	28	1.64	1.54
		28	1.52	1.50
4	1x1	42	1.08	1.79
		42	1.09	1.87

Proposal ID 11848 : CCD Read Noise Monitor Program

Purpose and Description of Program	The goal was to monitor the growth and fluctuations of the read noise for gain 1 and 4 with binnings 1x1, 1x2, 2x1, and 2x2 read out through each amplifier.
Execution	The execution of the program was nominal. 2 visits of 16 exposures occurred per month from August 2009 to November 2009 and for the rest of the cycle the same set of 2 visits were taken every other month. No changes were made to the program.
Summary of Analysis	Pairs of bias frames were used to measure the read noise by measuring the rms dispersion in a difference image cleaned of discordant pixels via iterative sigma clipping. Batch mode programs were used to make the measurements and produce cumulative tables and plots for the STIS calibration monitor webpage **(http://www.stsci.edu/hst/stis/performance/monitoring/)**. Two example plots are shown in Figures 4 and 5. These figures show the read noise for the entire history of STIS. Read noise values have stayed essentially the same since the SM4 repair. There has been an $\approx$ 0.2 DN increase (from $\approx$ 5.4 DN to $\approx$ 5.6 DN) in the read noise for gain = 1, 1x1 binning between STIS failure in 2004 and its repair in 2009. During this same period of time the read noise for gain = 4, 1x1 binning increased $\approx$ 0.1 DN (from $\approx$ 1.9 DN to $\approx$ 2.0 DN).
Accuracy Achieved	The errors in the gain 1 1x1 binning read noise have become larger because of the pattern noise generated by the Side-2 electronics and the increase in damage to the CCD by cosmic rays. The error for amplifier D, gain 1, 1x1 binning was estimated to be $\approx$ 0.14 DN and $\approx$ 0.03 DN for amplifier D, gain 4, 1x1 binning.
Continuation Plans	This calibration program has been continued in Cycle 18 as an amalgamation of the Read Noise Monitor and Bias Monitor (programs 12402 and 12403).

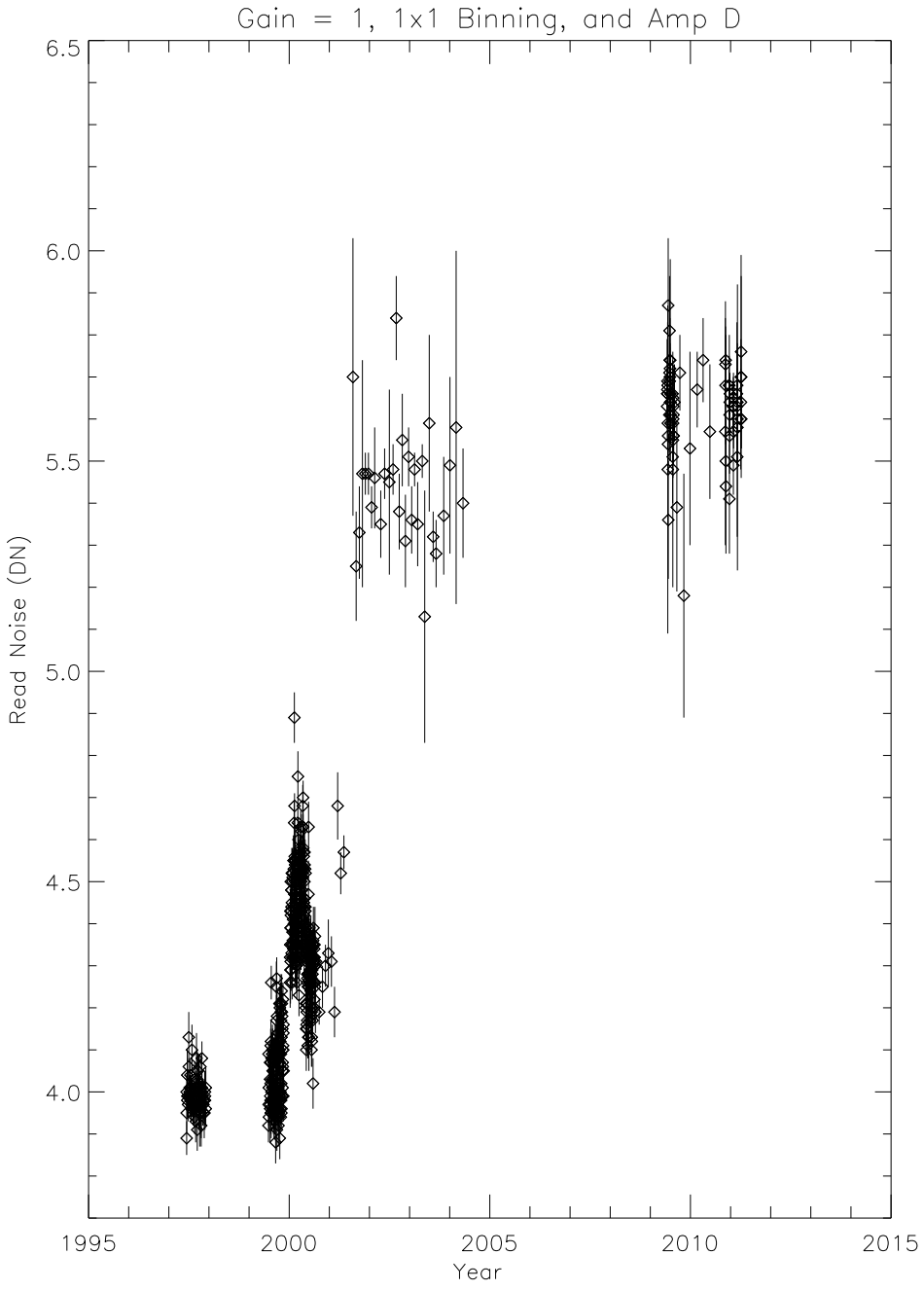

Figure 4. Read Noise history for STIS at gain = 1 and 1x1 binning settings.

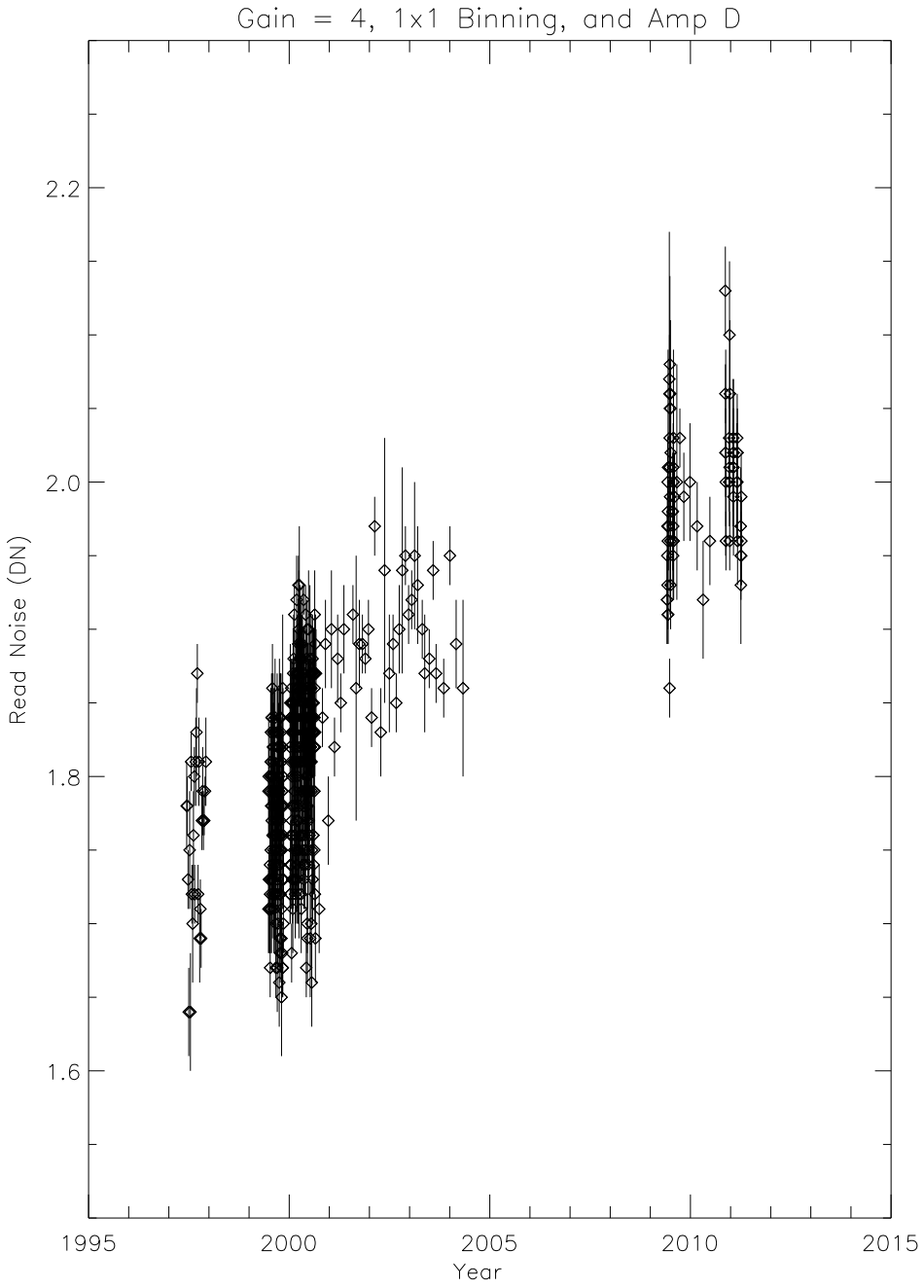

Figure 5. Read Noise history for STIS at gain = 4 and 1x1 binning settings.

Proposal ID 11849: CCD Annealing Program

Purpose and Description of Program	The goal of the program was to anneal hot pixels and monitor the growth of hot pixels by examining pre- and post-anneal dark images.
Execution	The execution of the program was nominal. The program was initially given 204 orbits which is the number required if not implemented in pure parallel mode. If done in pure parallel mode only 85 orbits are needed for the anneal program to be successful.
Summary of Analysis	Figures summarizing the anneal results are posted monthly on the STIS monitors page **http://www.stsci.edu/hst/stis/performance/monitoring/**. Since the Side-2 electronics do not contain a working temperature control circuit for the CCD, the data are scaled to a common CCD housing temperature before statistics are computed. During Cycle 17, the number of post-anneal hot pixels at the level of 0.1 e-/s increased from 33834 to 43444. Even after scaling all darks to a common temperature, the number of hot pixels measured above a given threshold fluctuates considerably as seen in Figure 6. The number of post-anneal hot pixels at the 0.1 e-/s level was as high as 50000 during this program. The median dark current for this same period varied between 0.00919 and 0.0146 counts/pixel/second. Average growth rate of hot pixels is $\approx$ 3.7% per month.
Accuracy Achieved	For post-SM4 data, the greater variation in the dark current makes it more difficult than it was for pre-SM4 data to determine the fraction of new hot pixels which are alleviated by the annealing process each month. The accuracy stated in the Phase I document is 1% for the growth rate. There is an ongoing investigation in the scatter inherent in the dark current. Since the number of hot pixels varies with the dark current it is difficult at this time to calculate a robust accuracy for the growth rate of hot pixels.
Continuation Plans	This program has been continued in Cycle 18 as program 12404.

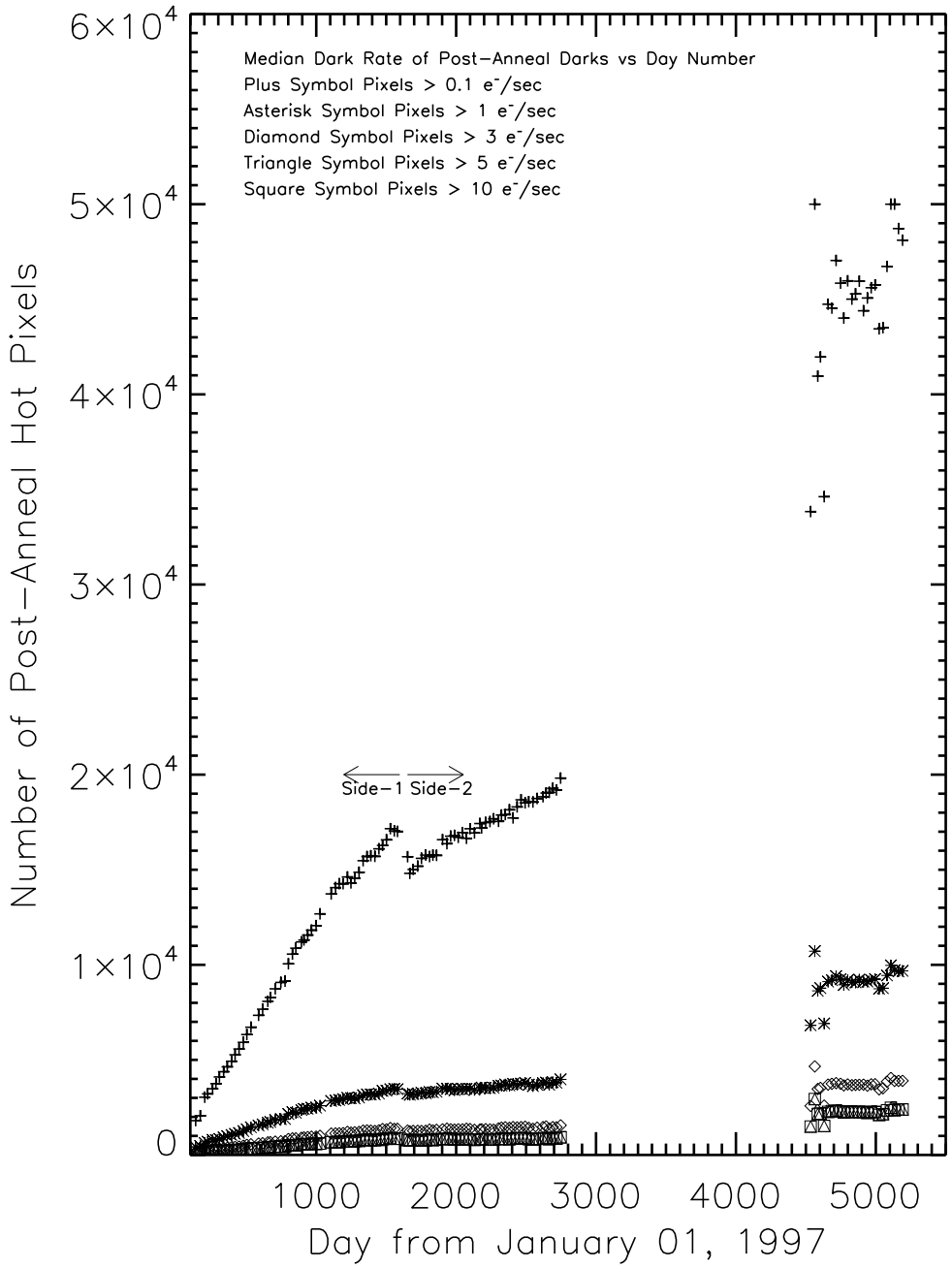

Figure 6. Number of hot pixels remaining after CCD anneals as a function of time for various count rate thresholds (see legend). The scatter in the first few data points, after SMOV4, is due to STIS being turned off and on for various reasons. The scatter in the remaining data points following SM4 is due to increased scatter potentially caused by individual pixels being less well behaved because of the accumulation of radiation damage.

Proposal ID 11850: CCD Charge Transfer Efficiency (Internal) Program

Purpose and Description of Program	The goal was to measure and establish an accurate correction for parallel register CTE losses via internal calibration lamp observations taken through narrow slits. Revised values for the CTE correction coefficients were to be put into the ccdtab reference files if necessary. The centroid shifts of the extraction regions in the y-direction (along columns) were reviewed as they have been in the past by Goudfrooij et al. (2006).
Execution	The execution of the program was nominal. Ten orbits were added to obtain biases in gain = 1 and 4 to create superbiases with a S/N greater than 1 using amps A and C.
Summary of Analysis	A sequence of nominally identical exposures is taken, alternating the read-out between amplifiers on opposite sides of the CCD. After correcting for gain differences in the read-out chains, the observed ratio of the fluxes seen by the two amplifiers can be fit to a simple model of constant fractional charge loss per pixel transfer. By fitting the observed flux ratio at a range of source positions along the columns, one can confirm that what is being measured is indeed a charge transfer effect. This internal sparse field test makes use of the on-board tungsten lamp and projects an image of a narrow slit at five positions along the CCD columns. At each position the read-out is alternated between amplifiers. For each exposure, the average flux per column within a standard 7-row extraction aperture and the centroid of the image profile within those 7 rows is calculated. The alternating exposure sequence allows CTE effects to be separated from warm-up effects of the calibration lamp. A revised value for the time dependence of the CTE was determined and put into the ccdtab reference file. The centroid shifts were observed to be directly propositional with CTI. For the very short exposure times the centroid shifts are large due to its dependance on signal levels. Short exposures have lower signal levels and smaller background.

Summary of Annalysis (cont.)	Figures 7 and 8 show the results from the charge transfer inefficiency (CTI) and centroid shift analysis. Note that the time dependence still follows a linear extrapolation as can be seen by the new data point plotted (last data point) in Figure 7. Note that the centroid shifts increase with decreasing signal as shown in Figure 8. For a full description of the Internal Sparse Field Test see Goudfrooij et al. (2006).
Accuracy Achieved	CTI values are accurate to within 1% for signal levels > 200 e-.
Continuation Plans	This calibration program has been continued into Cycle 18 as program 12408.

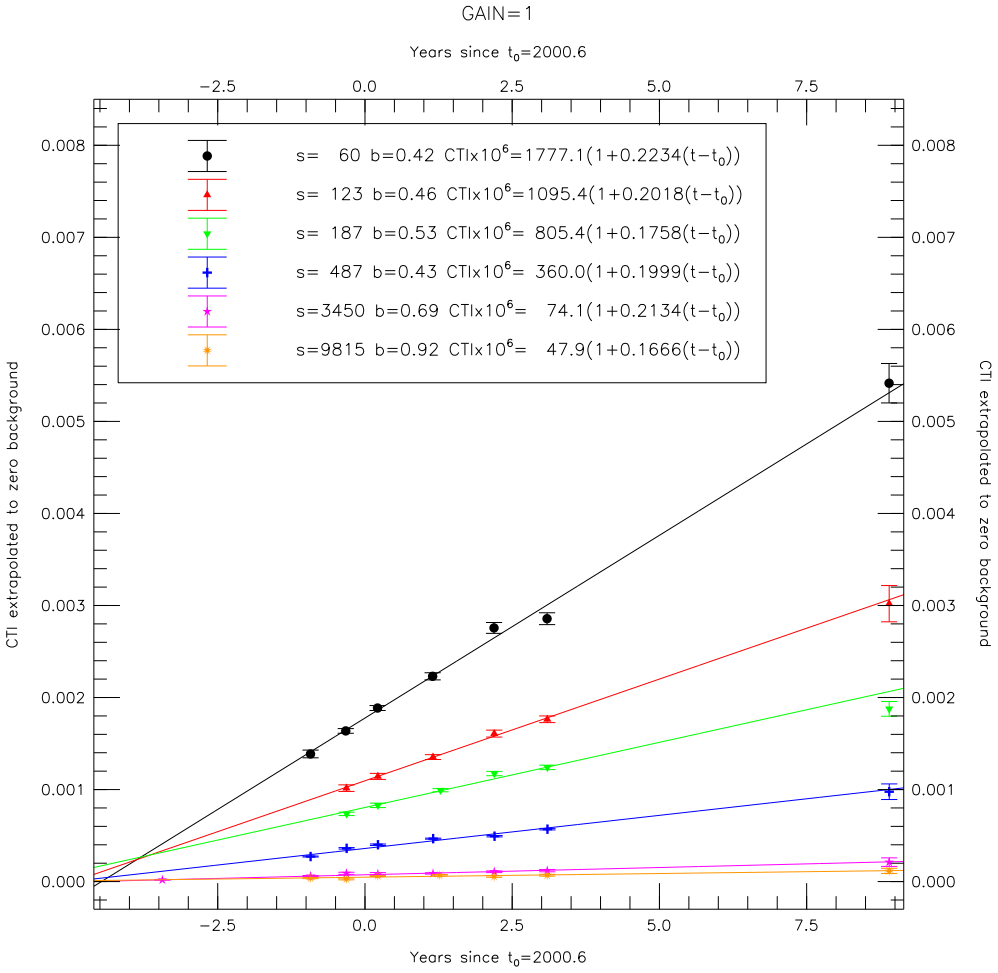

Figure 7. CTI as a function of time. The value for the source and background can be found in the legend and is denoted as "s" for the source and as "b" for the background.

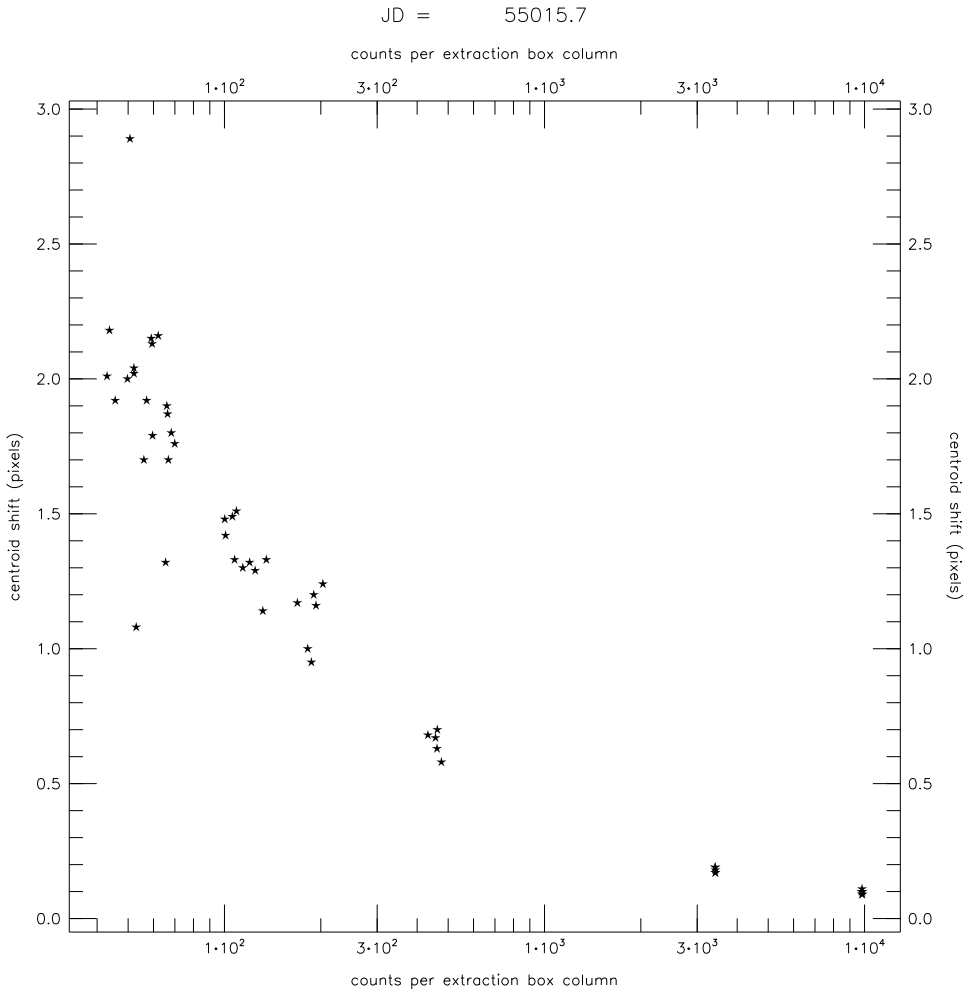

Figure 8. Centroid shift as a function of signal level.

Proposal ID 11852: CCD Spectroscopic Flats Program

Purpose and Description of Program	The goal was to obtain CCD flats on the STIS CCD in spectroscopic mode and to determine the pixel-to-pixel variations for spectroscopic observations.
Execution	Execution of the program was nominal. Observations were front-loaded to inspect any possible changes that might have occurred since the failure of STIS or during the SM4. 22 out of 50 visits executed in August 2009, while 11 visits executed in April 2010. The rest of the visits took place with a rate of two visits per month on average.
Summary of Analysis	New pixel-to-pixel at (P-flat) field reference files were created during the analysis. They were tested using high signal-to-noise data where targets had been dithered along the slit so that the spectral stripes have been recorded at different places on the detector. The testing showed that the new P-flats can reduce the residual scatter and the RMS deviation up to about 20 per cent in comparison to the old reference files when spectra recorded at different dither positions were compared. The new P-flats were also tested against calibration without any flat field correction. No spurious features were detected when the new P-flats were used. During the testing the new P-flat reference files were found to have only a modest impact on the signal-to-noise ratio of the extracted 1-dimensional spectra. In December 2009 the new P-flat field reference files were delivered to the CDBS and adopted for pipeline calibration. Additionally, new Python based software to generate STIS spectroscopic P-flats was written and introduced in Niemi (2010) and Niemi et al. (2010).
Accuracy Achieved	Less than 1 per cent accuracy for the residual scatter was achieved, in agreement with the goal set in the Phase I.
Continuation Plans	The program has been continued in Cycle 18 with program 12405.

Proposal ID 11853: CCD Imaging Flats Program

Purpose and Description of Program	The goal was to investigate STIS CCD flat-field stability over a monthly period.
Execution	Execution of the program was nominal. Observations were front-loaded to inspect any possible changes that might have occurred since the failure of STIS. Three out of 12 visits executed in August 2009. The following visits executed on average every second month.
Summary of Analysis	The CCD flat-field data were compared against old data and the reference files currently used in the pipeline processing. Small changes (generally less than 1%), for example in the dust motes, were noted when comparing the post SM4 data to the flat fields currently in CDBS. In only a few occasions the changes were noted to be larger than 1%. Since the STIS CCD has an RMS of 0.8% (Bohlin 1999) changes $\gg$ 1.0% could be relevant and should require further analysis. The amount of data collected did not allow the generation of a new high signal-to-noise flats, which would show improved calibration over the old flat fields. No pinholes or other defects were noted. Further information can be found in Niemi et al. (2010).
Accuracy Achieved	The accuracy achieved was slightly less than anticipated in the Phase I. The illumination of the calibration lamps are relatively uneven when taking imaging flat fields, thus, slightly lower signal-to-noise was achieved on regions that see less light. There has been no change since SM4.
Continuation Plans	The program has been continued in Cycle 18 as program 12406.

Proposal ID 11854: CCD Full-Field Sensitivity Monitor Program

Purpose and Description of Program

The goal was to annually monitor the CCD sensitivity over the whole field of view by measuring a photometric standard star field in Omega Cen in 50CCD annually to monitor CCD sensitivity over the whole field of view. This test allows a direct comparison of the 50CCD magnitudes to the Johnson-Cousins system for red sources. These transformations should be accurate to 1%. The stability of these transformations has been measured to the sub-percent level. These observations were supposed to provide a check of the astrometric and PSF stability of the instrument over its full field of view. In reality, we only checked the photometric stability, as described below.

Execution

There were no problems with observations. This program is executed once annually.

Summary of Analysis

The analysis used all of the 60-second exposures of the target field taken since 2000 and in particular the sx2.fits files, which are fully reduced, including corrections for cosmic rays and geometric distortion. Photometry was performed using the IRAF program PHOT, which requires as input the value ZMAG = -2.5 log(PHOTFLAM) - 21.10. Additionally, all processed datasets are corrected for time-dependent sensitive through the pipeline. 5-pixel apertures were used and then magnitudes were corrected for aperture losses. A correction for CTE effects was accomplished using the CTESTIS routine in IRAF.
From the eighteen stars in the sample with STMAG < 19, a mean sensitivity decline of $1.29 \pm 0.87\text{x}10^{-4}$ mag per year was derived. Over ten years, that comes to 1.3 millimag, or a throughput loss of 0.12%. For the entire sample (STMAG < 21.7), the sensitivity change is consistent with zero.

Accuracy Achieved

According to the analysis, the CCD photometry has drifted by less than 0.12% over ten years, well within the 1% requirement.

Continuation Plans

This program has been continued in Cycle 18 as the program 12409.

Proposal ID 11855: CCD Spectroscopic Sensitivity Monitor Program

Purpose and Description of Program	The goal of this calibration program was to monitor the spectroscopic sensitivity of the CCD, in order to update the time-dependent sensitivity reference files. Another goal was to monitor the STIS focus in imaging mode.
Execution	The program executed without any problems. The low resolution CCD modes were observed every month for 3 months, then once every 4 months after that. The M-modes were each observed twice. A total of 10 orbits were used in this program.
Summary of Analysis	Six visits monitoring the low-resolution modes were examined. The time dependent sensitivity (TDS) trends were updated in a reference file based on SMOV4 and initial Cycle 17 results on September 10, 2009. The trends observed during the rest of Cycle 17 showed a continuation of these values as is shown in Figures 9, 10, and 11 (note that the red symbols denote data taken at the E1 position on the CCD). Information can also be found in Proffitt et al. (2010). The focus data was not analyzed.
Accuracy Achieved	The accuracy required was a minimum S/N of 50 at the wavelength of least sensitivity, and this was achieved.
Continuation Plans	This program has been continued in Cycle 18 as program 12411.

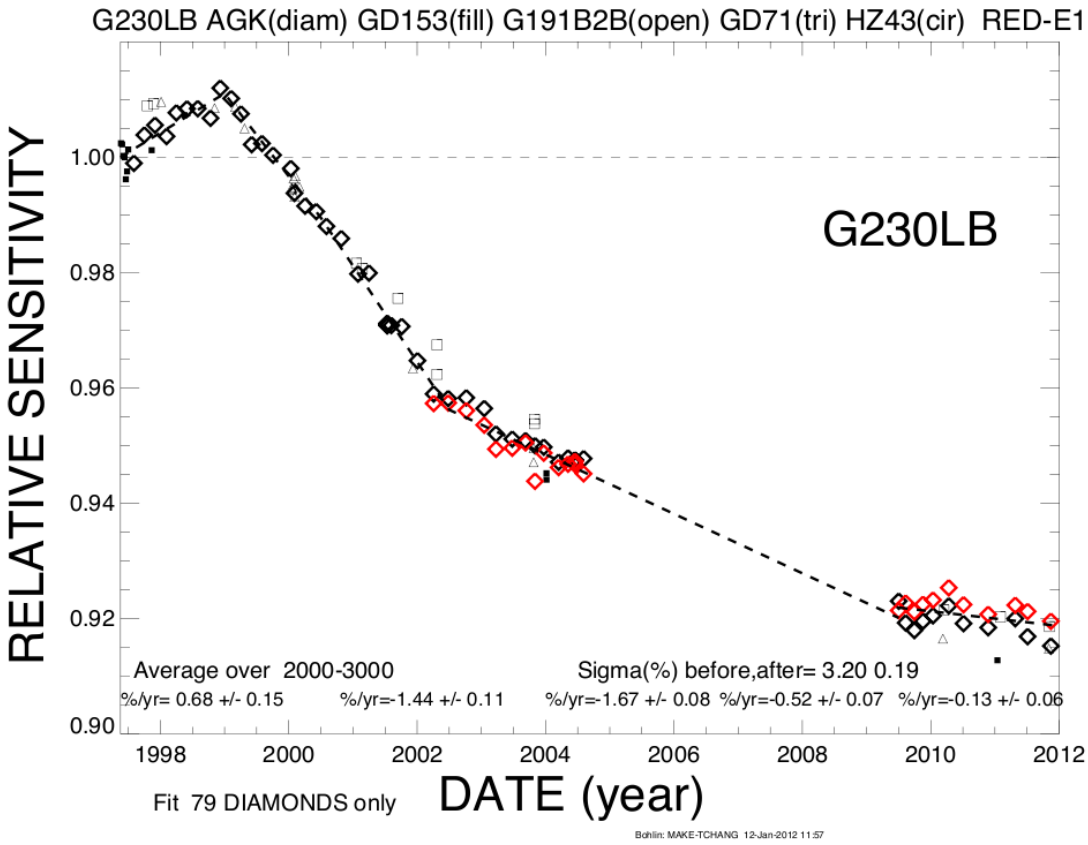

Figure 9. Plotted is the relative sensitivity as a function of time for the grating G230LB. The red symbols represent data taken at the E1 position.

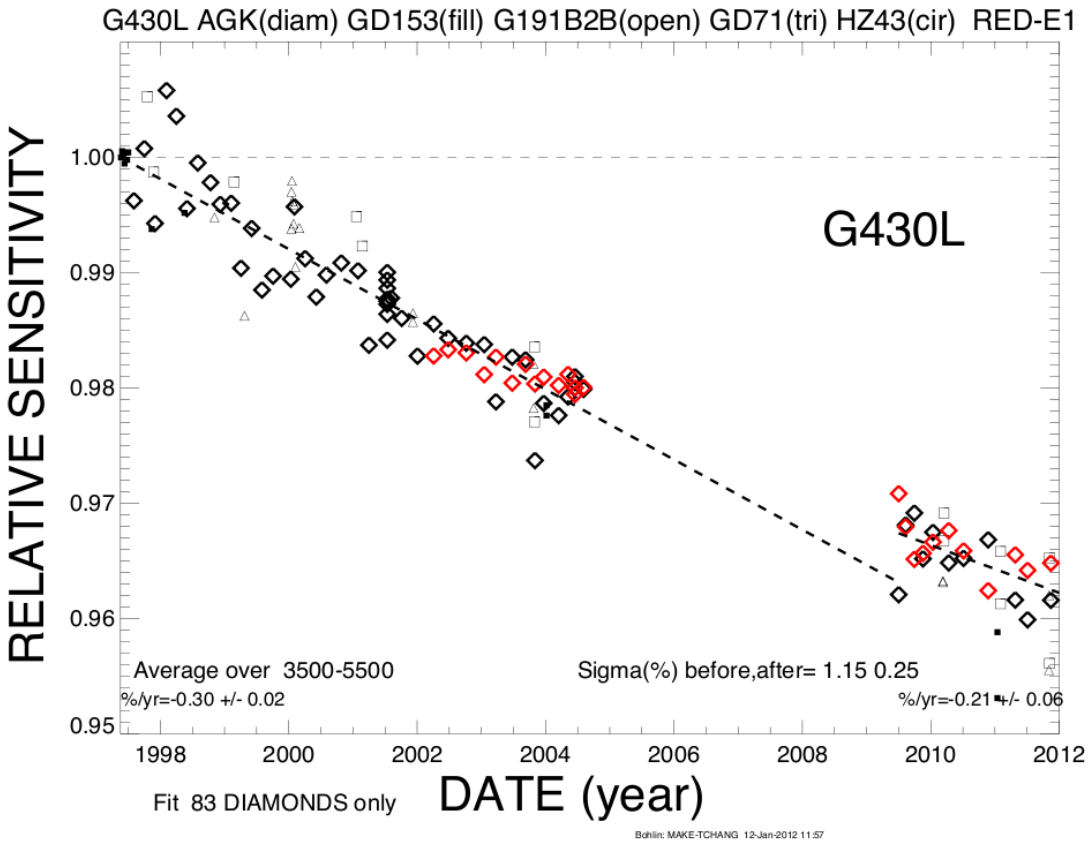

Figure 10. Plotted is the relative sensitivity as a function of time for the grating G430L. The red symbols represent data taken at the E1 position.

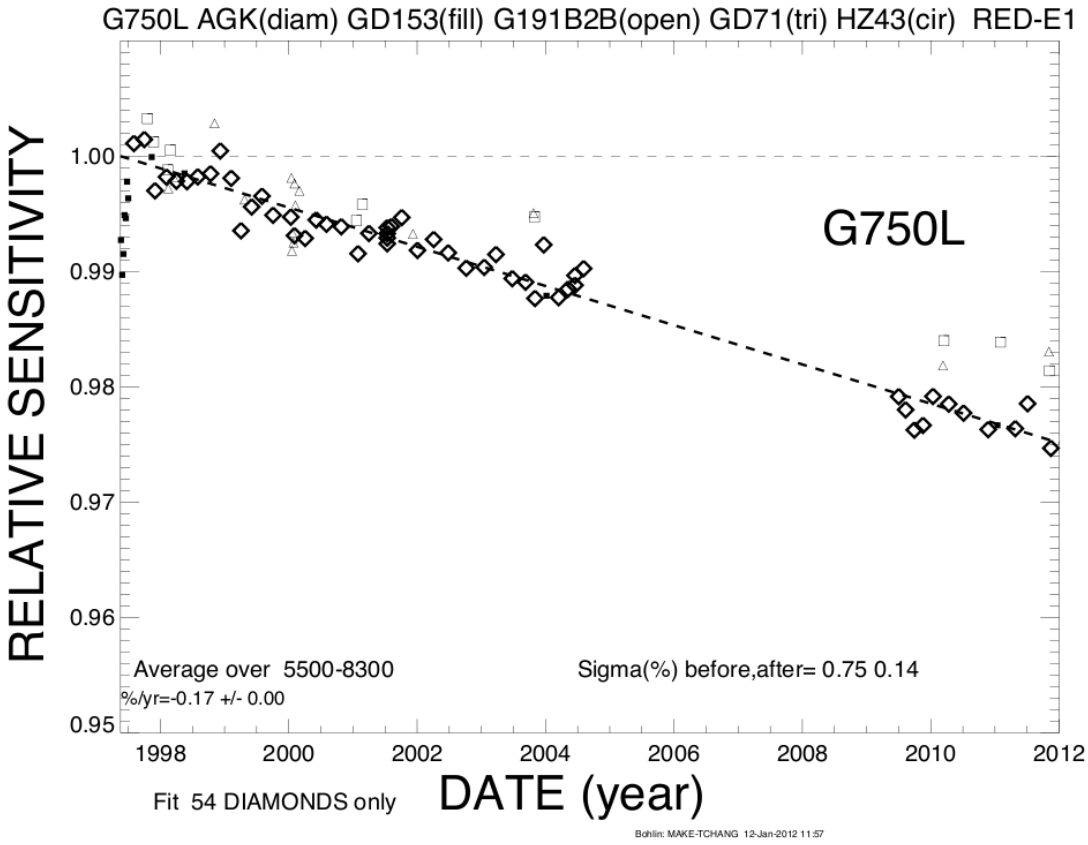

Figure 11. Plotted is the relative sensitivity as a function of time for the grating G750L.

Proposal ID 11858: CCD Dispersion Solution Program

Purpose and Description of Program	The goal was to investigate whether there are any changes in the STIS CCD dispersion solutions after SM4.
Execution	There were no problems in execution. This is an annual monitoring program.
Summary of Analysis	For all 39 settings, comparisons of the location of observed line spectra with catalogued Pt/Cr-Ne lines from the original compilation of Don Lindler as well as new compilations of Pt/Cr-Ne lines were performed. IDL routines were created to automate the line identification and fitting and have diagnostic plots such as line identified versus catalogued lines and differences between observed and catalogued lines as a function of wavelength and setting. The wavelength zero-point accuracy quoted is the mean of the differences between observed and catalogued lines over a setting. The relative wavelength accuracy quoted is the standard deviation of the differences between observed and catalogued lines over a setting. An ISR summarizing this analysis has been written and is published (Pascucci et al. 2010).
Accuracy Achieved	The typical accuracy for the wavelength zero-points is 0.1 pixels while for the relative wavelength it is 0.2 pixels. These accuracies compare well with pre-SM4 accuracy.
Continuation Plans	This calibration program has been continued as program 12407 in Cycle 18.

4. MAMA Monitoring and Detector Calibration

Proposal ID 11856: MAMA Full-Field Sensitivity Monitor Program

Purpose and Description of Program	The purpose of this program is to monitor the sensitivity of the MAMA detectors over the full field. This is achieved by observing the globular cluster NGC 6681 annually. The data can be compared with those from Cycles 7, 8, 9, 10, 11, and 12.
Execution	There were no problems with observations. This program is executed once annually.
Summary of Analysis	The STIS NUV- and FUV-MAMA detectors are used for both imaging and spectroscopy. We use observations of the globular cluster NGC 6681 to conduct two tests of the MAMA full-field sensitivity. First, we compare photometry obtained during Cycle 17 with that from previous cycles to track temporal changes in the detector sensitivity. Second, we compare the photometry of stars observed in all four quadrants of each detector to look for spatial variations in the sensitivity. In both tests, we find that the observed trends are far smaller than the 5% uncertainty quoted for both absolute and relative photometry with the STIS NUV- and FUV-MAMA.
Accuracy Achieved	TDS changes uncorrected by CALSTIS come to less than 1.5% over a ten-year period. Measured spatial variations are consistent with uniform sensitivity, but the data suggest a small variation in sensitivity across the detector. Any such trends are less than the 5% quoted uncertainty in STIS MAMA photometry.
Continuation Plans	This program has been continued in Cycle 18 as 12413.

Proposal ID 11857: MAMA Darks Monitor Program

Purpose and Description of Program	This proposal monitors the behavior of the dark current in each of the MAMA detectors for the production of reference files.
Execution	Two exposures for each STIS MAMA detector were taken weekly. For the FUV-MAMA detector, six additional exposures were taken once every six months to gain information on the dark rates as a function of the amount of time that the HV has been on. Between September and October 2010 the STIS MAMA detectors were shut down. All visits scheduled to execute during this period of time were withdrawn. Therefore, only 106 out of the 288 allocated orbits were executed.
Summary of Analysis	The NUV-MAMA dark rate has varied considerably over Cycle 17, mainly following a pattern of decline with a characteristic time scale of more than 500 days. See Figure 12 for a plot showing the time dependence of the NUV dark current. As of October 31, 2010, the dark current level is about 2.5 times that seen in 2004. A dark reference file and a TDC file were delivered in December 2009 for the NUV. The FUV-MAMA dark rates are essentially the same as before SM-4 and were stable throughout the calibration cycle. For an in-depth analysis of the MAMA dark current and a full description of the curve fitting seen in Figure 12 see Proffitt et al. (2010), Zheng et al. (2010), and Zheng, Proffitt, & Sahnow (2011).
Accuracy Achieved	The new NUV TDC file enables a dark subtraction to an accuracy of < 0.0005 count/sec/pixel. The FUV dark current ≈ 0.00005 count/sec/pixel.
Continuation Plans	The program has been continued in Cycle 18 as 12415.

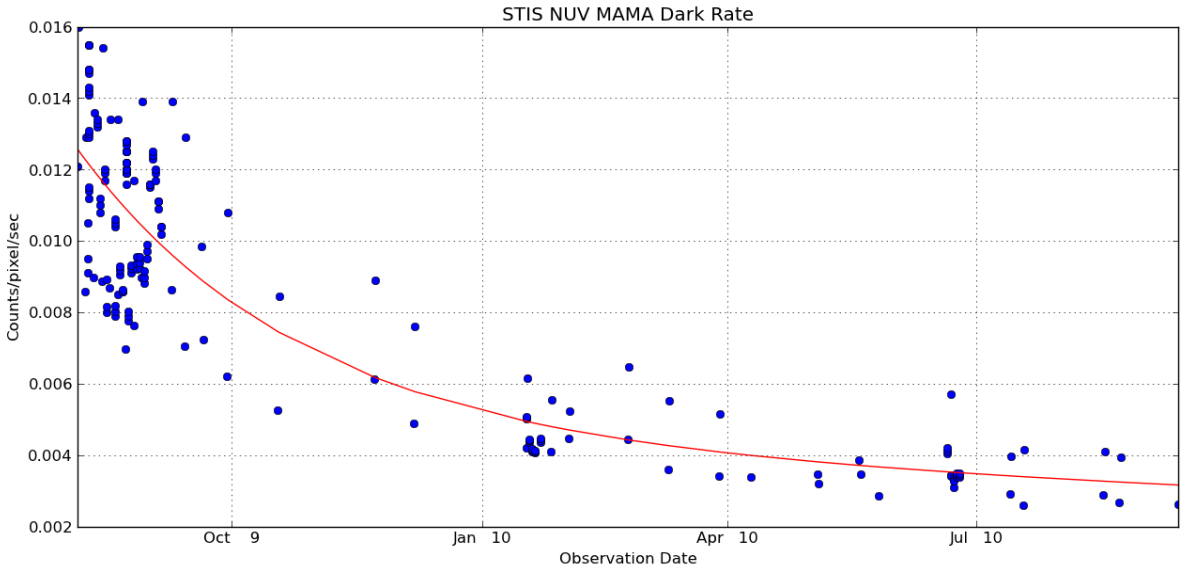

Figure 12. The STIS NUV-MAMA dark rate since SM4. Blue filled circles are measurements of the dark current. The red curve is the model fit with dual exponential components.

Proposal ID 11859: MAMA Dispersion Solution Program

Purpose and Description of Program	The goal was to investigate whether there are any changes in the STIS MAMA dispersion solutions after SM4.
Execution	There were no problems in execution. This is an annual monitoring program.
Summary of Analysis	For all 26 settings, comparisons of the location of observed line spectra with catalogued Pt/Cr-Ne lines from the original compilation of Don Lindler as well as new compilations of Pt/Cr-Ne lines were performed. IDL routines were created to automate the line identification and fitting and to have diagnostic plots such as lines identified versus catalogued lines. The routines also estimate the differences between observed and catalogued lines as a function of wavelength and setting. The wavelength zero-point accuracy quoted is the mean of the differences between observed and catalogued lines over a setting. The relative wavelength accuracy quoted is the standard deviation of the differences between observed and catalogued lines over a setting. An ISR summarizing this analysis has been written and published (Pascucci et al. 2010).
Accuracy Achieved	The typical accuracy for the wavelength zero-points is 0.1 pixels while for the relative wavelength is 0.2 pixels. These accuracies compare well with pre-SM4 accuracy.
Continuation Plans	This calibration program has been continued in Cycle 18 as program 12412.

Proposal ID 11860: MAMA Spectroscopic Sensitivity and Focus Monitor Program

Purpose and Description of Program	The main goal of the program was to monitor the spectroscopic sensitivity. A secondary goal was to monitor the STIS focus in a spectroscopic and an imaging mode.
Execution	Visit 2 of this program failed, and was repeated in visit N2. Visits 01, 06, and X2 were withdrawn. The program consists of multiple visits: the low-resolution modes were observed every 1-3 months, the medium-resolution modes once, the prism once, and the echelle modes initially every 6 months. Inspection of the first echelle visit revealed a throughput anomaly in the E140H data, and the monitoring frequency was increased to a total of 4 visits for this program (monitoring frequency doubled). The last visit of the echelle monitoring and the last visit of low-resolution monitoring did not occur, due to timing: the MAMAs were placed in an inhibit state starting in September 2010 due to problems encountered during an SIC&DH event. When the MAMAs were turned back on, these visits were withdrawn and the Cycle 18 monitoring program commenced. A total of 16 orbits were allocated in this program but only 14 were executed including the repeat of Visit 2.
Summary of Analysis	Updated time-dependent sensitivity reference files were delivered for the FUV on July 12, 2010, and for the NUV on November 9, 2010. The throughput anomaly observed early in E140H appeared to have recovered by June 2010. Figures 13 and 14 show the relative time dependent sensitivity as a function of time. Note that the trend for G140L appears to be following data taken before SMOV4, whereas the G230L trend changes for data taken after SMOV4. The STIS MAMA focus data was not analyzed.

Accuracy Achieved The accuracy required in the phase I was a minimum SNR of 50 at the wavelength of least sensitivity for the L modes, and at the central wavelength of the M and E modes. The minimum SNR was met over the wavelength range 1235-1545 Å for the G140L, and again near 1165 Å; for the G230L it was met over the wavelength range 1730-2970 Å. For the M and E modes, the SNR at the central wavelength was between 35 and 40 per pixel.

Continuation Plans This program has been continued in Cycle 18 as program 12414.

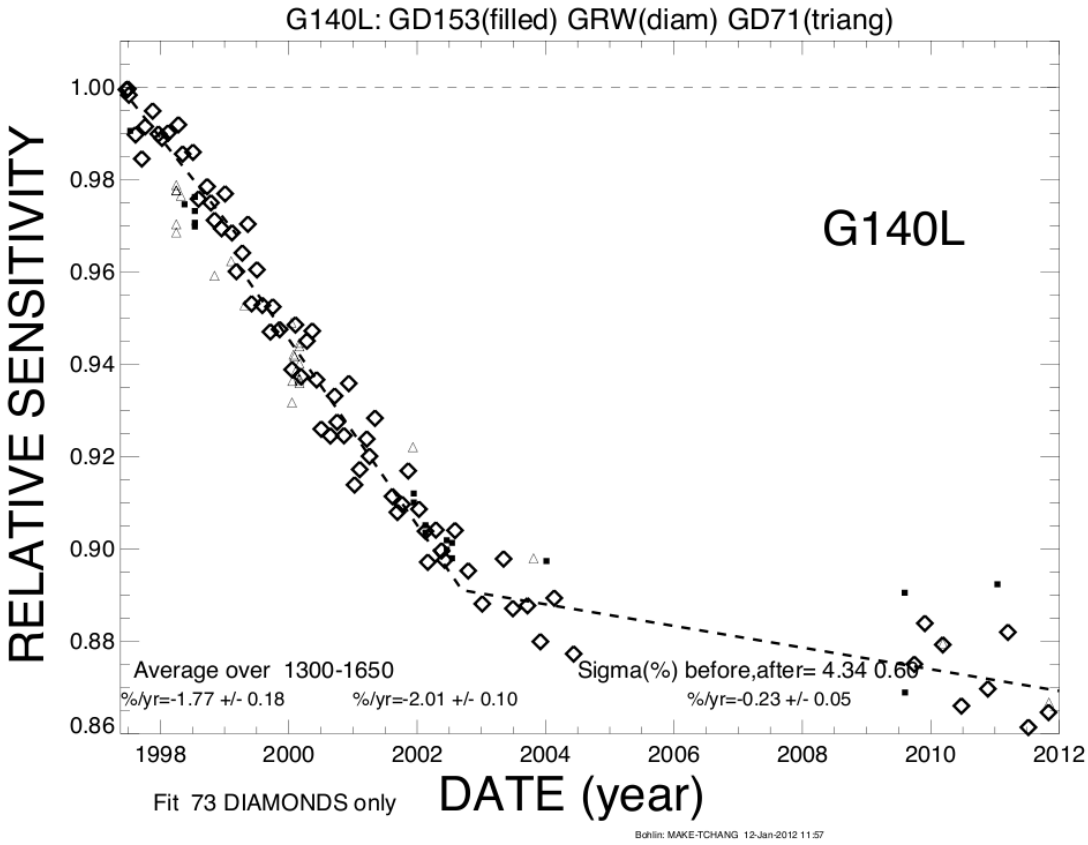

Figure 13. Plotted is the relative sensitivity as a function of time for the grating G140L.

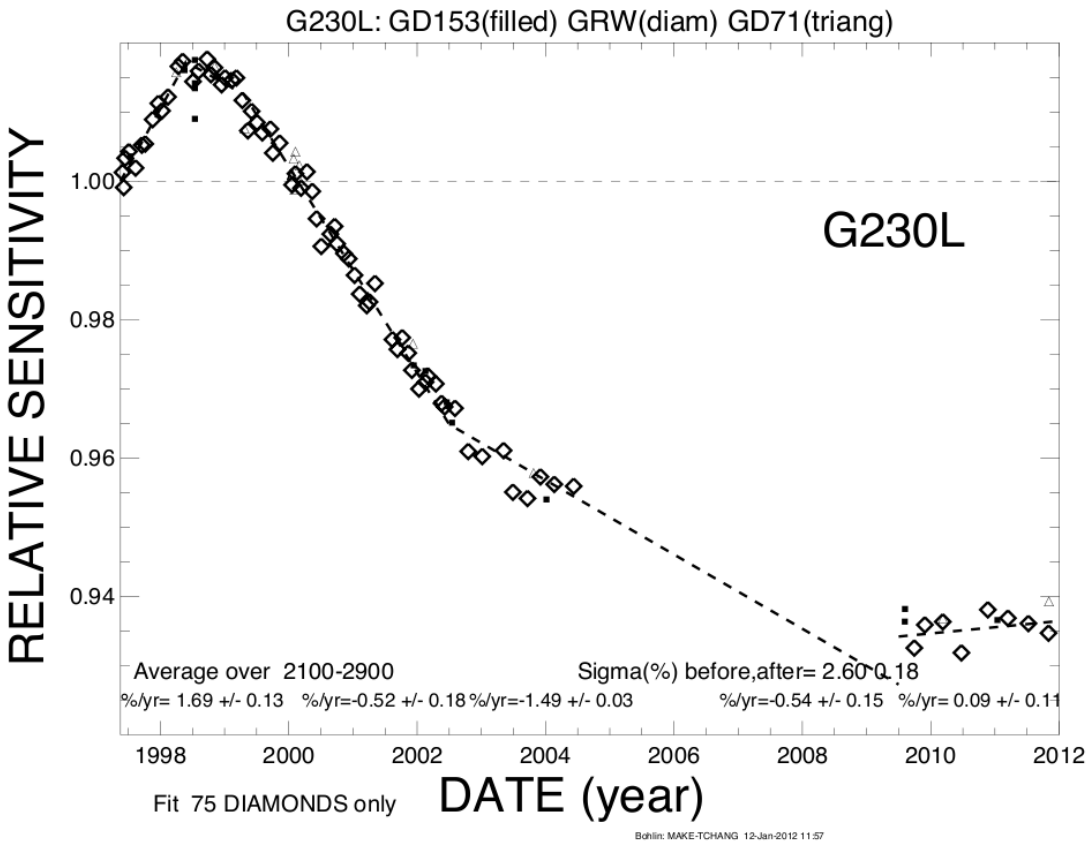

Figure 14. Plotted is the relative sensitivity as a function of time for the grating G230L.

Proposal ID 11861: MAMA FUV Flats Program

Purpose and Description of Program	The goal was to determine the pixel-to-pixel response (p-flat) of the FUV detector, applicable to all FUV modes. Following Brown & Davies (2002) recommendations the FUV and NUV MAMA flat field programs have been reduced in frequency and are executed just for monitoring purposes to check the evolution of the flat field.
Execution	All planned exposures were successfully executed. Two exposures initially failed (visits 05 and 06) but HOPRs were filed and the exposures re-taken with no failures. Visits 05 and 06 were lost during the high voltage ramp up of the STIS FUV MAMA, the count rate limit was violated and a flag was set to prevent the detector from coming on again. This event happened while HST was brushing the northwest edge of the SAA, which was believed to be the cause of the high count rate. Due to the count rate violation, the detector was off while the planned visits executed. The failure had nothing to do with the actual observations. These two observations were scheduled about 24 hours apart, and the recovery of the FUV MAMA took nearly two days, so both were lost. These visits were re-observed as visits 55 and 56, respectively and both visits executed nominally. Also, three additional exposures were added as a supplemental calibration program giving a total of 14 visits.
Summary of Analysis	Software was revived and updated for the analysis of the p-flat data. This software (Brown & Davies 2002) was used to create and analyze all of the p-flat data from Cycles 7, 8, 9 10, and 11 creating a super p-flat for each calibration cycle where appropriate. These calibration cycle p-flats were then compared against each other and the current reference p-flat file to determine if there are any time dependent features. None were found. The same analysis was done when a p-flat was created from Cycle 17 calibration data and no time dependent features were discovered. The S/N of the p-flat created from Cycle 17 data was determined and found to be less than the S/N of the currently incorporated reference pipeline p-flat. Therefore, no new p-flat reference file was delivered. Data from Cycle 18 observations need to be employed in order to increase the S/N. Further information can be found in Niemi et al. (2010).

Accuracy Achieved	The total signal collected in 17 exposures is 3393 ADU (Poisson statistic) corresponding to a S/N = 58.25 $\pm$ 0.018 per pixel in high resolution mode. In low resolution mode this corresponds to a S/N = 116.5 $\pm$ 0.0086 per pixel.
Continuation Plans	This proposal has continued in Cycle 18 as program 12417.

Proposal ID 11862: MAMA NUV Flats Program

Purpose and Description of Program	The goal was to determine the pixel-to-pixel response (p-flat) of the NUV detector, applicable to all NUV modes and to compare with the response derived in previous cycles to look for time dependence. The program was also designed to co-add with data from previous cycles to improve S/N in the reference file, if warranted. Following Brown & Davies (2002) recommendations the FUV and NUV MAMA flat field programs have been reduced in frequency and are executed just for monitoring purposes to check the evolution of the flat field.
Execution	All planned exposures were successfully executed. 2 of which failed (visits 03 and 04) and were repeated successfully. Visit 03 failed because of a MAMA2 MCE reset, which turned off the high voltage before the observation started, so the detector was off at the time of the exposures. Visit 04 was lost in the SIC&DH reset a few days after the failure of visit 03.These visits were re-observed as visits 53 and 54, respectively and both visits executed nominally. Additionally, 1 of the 11 valid frames shows vertical bright structures/lines on the right side of the detector. This frame (obbl01elq_raw.fits) should not be used in any future p-flat creation.
Summary of Analysis	Software was revived and updated for the analysis of the p-flat data. This software was used to create and analyze all of the p-flat data from Cycle 11 creating a super p-flat. When the current reference file p-flat is compared to p-flat created from Cycle 17 calibration data there is a shift in the Moire pattern but since the Moire pattern is at the sub-pixel level there should be no problems due to the shift in the Moire pattern. The S/N of the p-flat created from Cycle 17 data was determined and found to be less than the S/N of the currently incorporated reference pipeline p-flat. Therefore, no new p-flat reference file was delivered. Data from Cycle 18 observations need to be employed in order to increase the S/N. Additional information can be found in Niemi et al. (2010).

Accuracy Achieved The total signal collected in 11 exposures is 2844.6 ADU (Poisson statistic) corresponding to a S/N = 53.33 $\pm$ 0.019 per pixel high resolution mode. In low resolution mode this corresponds to a S/N = 106.7 $\pm$ 0.0094 per pixel.

Continuation Plans This proposal did not finish executing in Cycle 18, but has been continued in Cycle 19.

Proposal ID 11866: MAMA Echelle Blaze Function Zero Points Program

Purpose and Description of Program

The goal was to calibrate the absolute sensitivity of all the primary and intermediate settings of the echelle modes on Side-2 operations after the STIS repair by using observations of the flux standard star G191B2B. While this was done in Cycle 10 (program 8915), the echelle blaze shift proved to depend sensitively on the side of operation employed, time, and the exact MSM positioning. We therefore obtained a complete set of post-repair data at the default MSM position to allow a comprehensive solution for the echelle blaze shifts on a repaired side 2.

Execution

All 5 visits were executed as planned in November and December 2009. The 5-orbit visit 03 executed on November 25, 2009 failed because of a guide star acquisition failure and was repeated on January 6, 2010 as visit 53. Exposures for this program were obtained in each of the primary and intermediate wavelength settings for the echelle modes E140H, E140M, E230H, and E230M. The program utilized a total of 24 orbits.

Summary of Analysis

Analysis of the data has been completes. FUV and NUV PHT reference files for flux calibration and a FUV and NUV RIP tables with updated blaze shape and position for the 2-D background subtraction algorithm, have been created and delivered. The analysis of this echelle data has also resulted in the update and delivery of the FUV and NUV Bad Pixel Tables. In both cases a column for each optical element was added to mark the repeller wire position (FUV) and the vignetted corners (NUV) that have been found to vary as a function of optical element. Bostroem et al. (2010) and Bostroem et al. (2012), describe in detail the new echelle flux calibration. A TIR to document the creation of the new PHT and RIP tables, and a TIR on the creation of the new NUV Bad Pixel table are also in preparation.

Accuracy Achieved The expected accuracy for the sensitivity curves describing the echelle blaze function should be better than 0.1% for the orders of all echelle primary and intermediate settings. These errors are well below other sources of error in the flux calibration procedure.

Continuation Plans Not continued. The evolution of the blaze shift as a function of time will be monitored through the MAMA sensitivity monitoring programs (Cycles 17, 18, 19 and 20, programs 11860, 12414, 12775 and 13145).

5. Operations, Engineering and Special

Proposal ID 11851: CCD Slit Wheel Repeatability Monitor Program

Purpose and Description of Program	The purpose was to test the repeatibility of the slit wheel at various positions.
Execution	One orbit of observations was executed as planned.
Summary of Analysis	Twenty four images were taken under a sequence. An IRAF script was used to find the relative shifts. A linear fit is made to remove the effect of time-dependent drifting. A 0.2 pixel offset was derived but this is less than the 0.5 pixel requirement and as a result slit wheel repeatability is nominal.
Accuracy Achieved	The test accuracy is 0.2 pixel, which is slightly better than the requirement of 0.5 pixel.
Continuation Plans	This program has been continued in Cycle 18 as program 12410.

Proposal ID 11863: MAMA Fold Distribution Monitor Program

Summary of Goals

Proposal 11863, the FUV and NUV detector fold tests, monitors the performances of MAMA microchannel plates. The fold analysis provides a statistical measurement of the distribution of charge cloud sizes incident upon the anode giving some measure of changes in the pulse height distribution of the MCP and, therefore, MCP gain as charge is extracted from the microchannel plate. The procedure is implemented using special commanding and is the same for the FUV- and NUV-MAMA with the exception of the gratings/aperture/lamp combinations used for the test. The results are presented separately starting with the FUV detector followed by the NUV.

Execution

All 4 visits executed, 2 each in November 2009 and May 2010. There were no anomalies with the observations.

Summary of Analysis

A brief description of steps used for the FUV detector follows. Set Software Global Monitor to SGM Threshold = 15000; SGM Integration period = 0.1 s. Begin a 2300-second HITM2 (Pt-Ne/Cr) MEDIUM (10 ma) lamp exposure with aperture F25ND3 and spectral element MIRROR. During the exposure, each fold is enabled separately and counters X, Y, Z, W, VE, EV, and OR are collected.

The engineering telemetry data was examined (voltages, currents, temperatures, relay positions, and status) for agreement with predicted values and previous ground and on-orbit test data all were nominal. The MAMA engineering telemetry event counter is also used to construct a histogram (Figure 15) of the number of counts for each fold. The results were compared and combined with the results from previous tests - again, all results were as expected, *i.e.,* there is a slight shift to higher folds as the detector ages. The combined results are shown below.

Summary of Analysis (cont.)

Post test, a dark exposure was taken where the counters were cycled and are plotted in a histogram (Figure 16). The dark count rate showed the typical low-count distribution and nothing out of the ordinary was observed.

A brief description of steps used for the NUV detector follows. Set Software Global Monitor to SGM Threshold = 15000, SGM Integration period = 0.1 s. Begin a 2300-second HITM1 (Pt-Ne/Cr) LOW (3.8 ma) lamp exposure with aperture F25ND3 and spectral element MIRROR. During the exposure, each fold is enabled separately and counters X, Y, Z, W, VE, EV, and OR are collected.

The engineering telemetry data was examined (voltages, currents, temperatures, relay positions, and status) for agreement with predicted values and previous ground and on-orbit test data all were nominal. The MAMA engineering telemetry event counter is also used to construct a histogram (Figure 17) of the number of counts for each fold. The results were compared and combined with the results from previous tests - again, all results were as expected, *i.e.,* there is a slight shift to higher folds as the detector ages. The combined results are shown below.

Post test, a dark exposure was taken where the counters were cycled and a histogram produced (Figure 18). Of interest is the decreasing dark count rate with time as each counter was sampled. Notice that post- SM4, series dated 09.212, the dark count rate was initially high. This was caused by 4.5 years of MAMA inactivity where the NUV-MAMA tube remained at approximately 1-2 degrees C and metastable states were allowed to accumulate in the MgF_2 window. The decrease seen after this has been attributed to the return of the MAMA to it normal operating temperatures of 29-33 degrees C and a reduction of long-term metastable states.

Accuracy Achieved

The FUV dark count rate showed nothing unusual, however, the NUV dark current initially showed a high dark current that has been decreasing with time.

Continuation Plans

This program has been continued in Cycle 18 as program 12416.

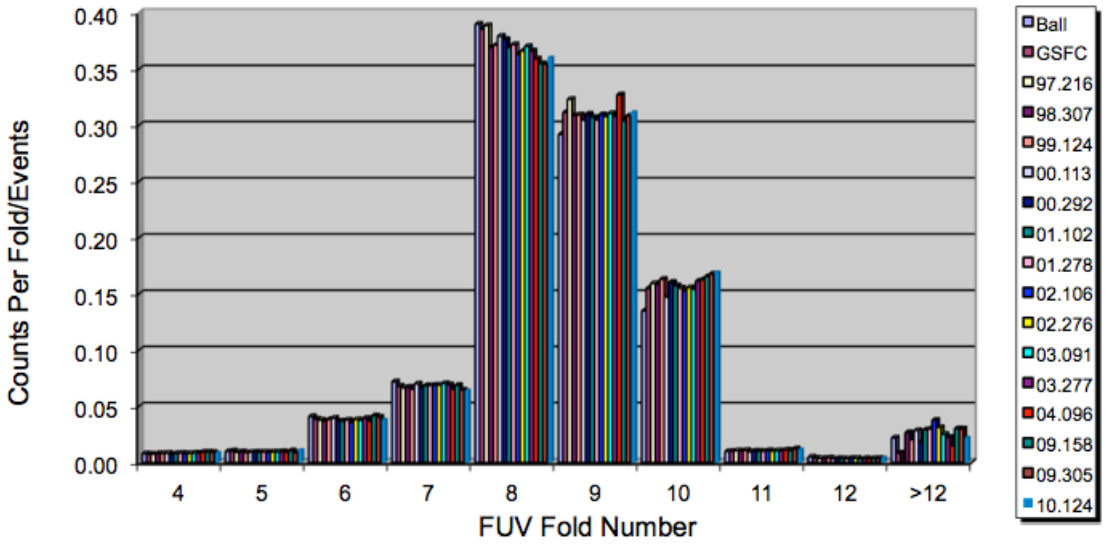

Figure 15. Histogram of STIS FUV Fold Test Results. The legend contains the date of the test and is interpreted as two digit year and day number of the year, e.g., yy.day number 10.124.

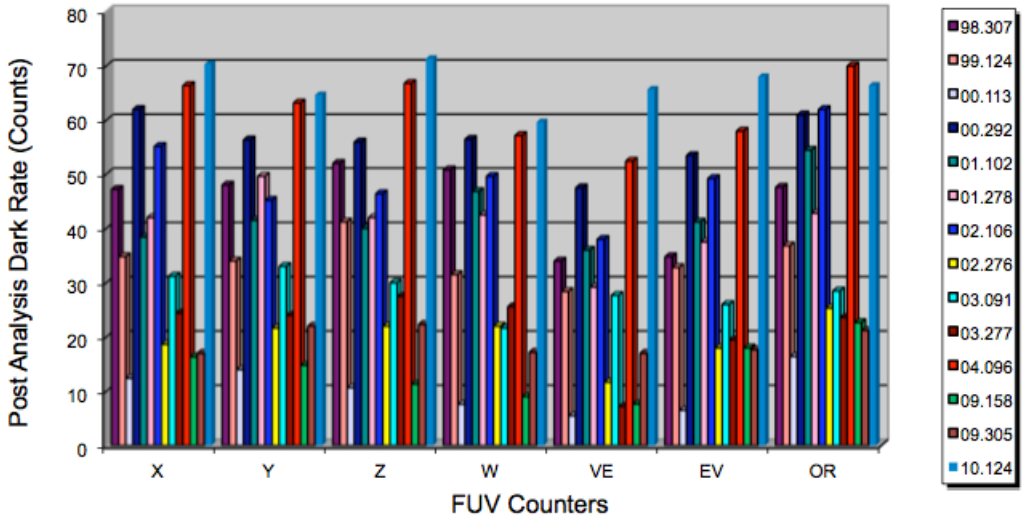

Figure 16. Post-test FUV showing typical dark count rates. The legend contains the date of the test and is interpreted as two digit year and day number of the year, e.g., yy.day number 10.124.

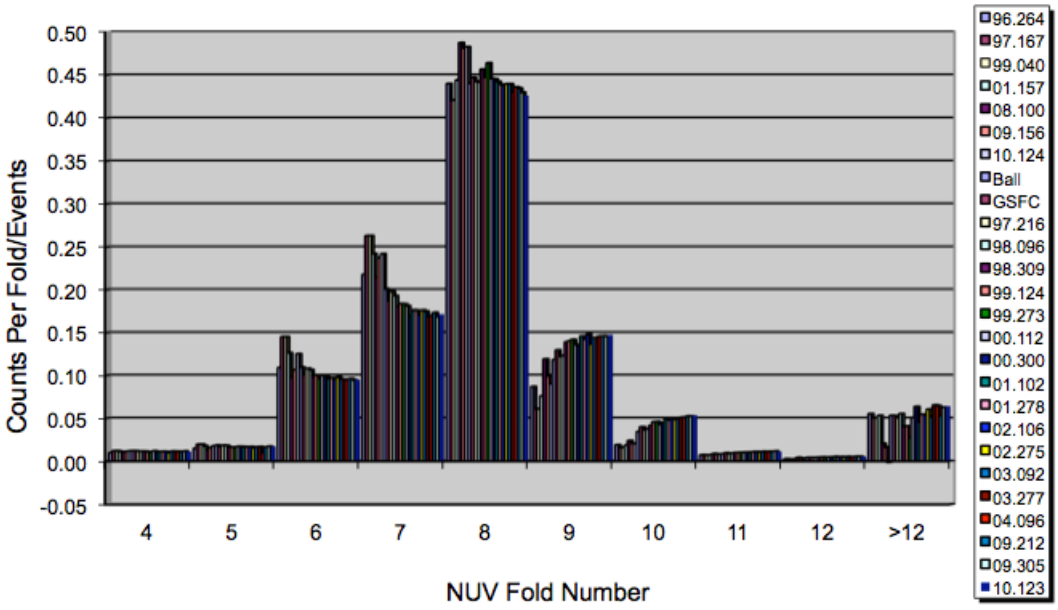

Figure 17. Histogram of STIS NUV Fold Test Results. The legend contains the date of the test and is interpreted as two digit year and day number of the year, e.g., yy.day number 10.124.

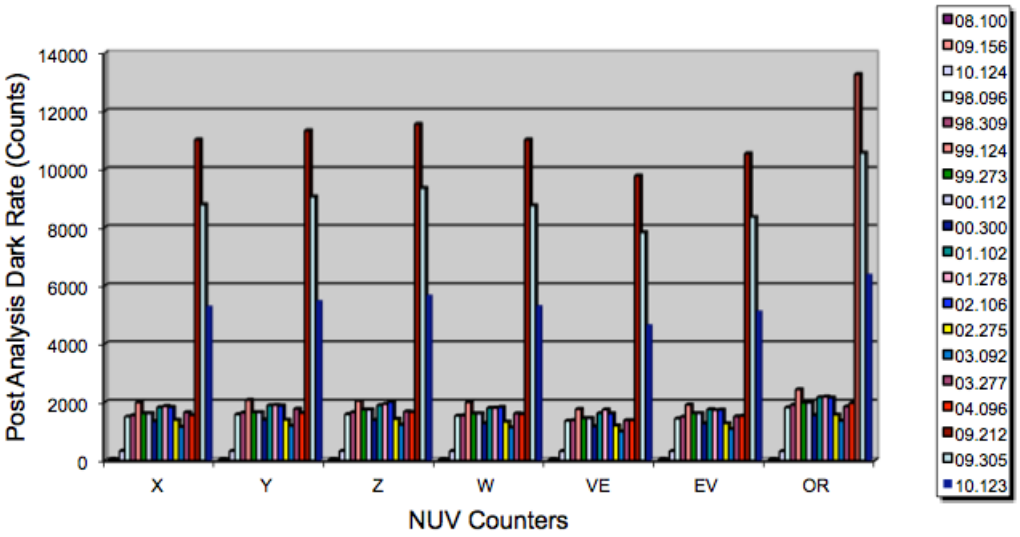

Figure 18. Post-test dark count rate showing the post-SM4 increase followed by a decreasing trend. The legend contains the date of the test and is interpreted as two digit year and day number of the year, e.g., yy.day number 10.124.

Proposal ID 11864: MAMA Anomalous Recovery Monitor Program

Purpose and Description of Program	Permit recovery of the FUV-MAMA or NUV-MAMA detector after an anomalous shutdown. Anomalous shutdowns can occur as a result of bright object violations which trigger the Bright Scene Detection or Software Global Monitors. They can also occur as a result of MAMA hardware problems.
Execution	Withdrawn. Not required during Cycle 17.
Summary of Analysis	N/A
Accuracy Achieved	N/A
Continuation Plans	This program has been continued in Cycle 18 as program 12429.

Proposal ID 11865: COS Flux Standard Monitor Program

Purpose and Description of Program	The purpose was the cross calibration of STIS and COS in the UV. Measurement and verification of CTE correction for the CCDs.
Execution	STIS observation of 2 orbits executed without problems.
Summary of Analysis	The STIS observations of LDS749B were fully reduced and the flux calibrated SED provided to support COS flux calibration. These flux models can be found in calspec.
Accuracy Achieved	The new fluxes were in agreement with previous STIS LDS749B fluxes to $\approx 1\%$. The extrapolation of the STIS CTE correction is also robust.
Continuation Plans	No more STIS observations are planned. LDS749B is a well verified faint flux standard.

Proposal ID 11652: CCD Throughput Calibration of the 52X0.2E1 Aperture Program

Purpose and Description of Program	N/A
Execution	The requested orbit was completed. This is a GO calibration proposal by S. Heap.
Summary of Analysis	N/A
Accuracy Achieved	N/A
Continuation Plans	N/A

Proposal ID 11999: JWST Calibration

Purpose and Description of Program	Recently, Gordon, Bohlin, et al. submitted a successful Spitzer proposal for cross calibration of HST and Spitzer. The cross-calibration targets are stars in three categories: WDs, A-stars, and G-stars. Traditionally, IR flux standards are extrapolations of stellar models that are tied to absolute fluxes at shorter wavelengths. HST absolute flux standards are among the best available with a solid basis that uses pure hydrogen models of hot WD stars for the SED slopes and is tied to Vega at 5556 Å via precise Landolt V-band photometry. Consistently matching models to our three categories of HST observations along with Spitzer photometry and the few existing absolute IR flux determinations will provide a solid basis for JWST flux calibration over its 0.8-30 micron range. The goal of this proposal is to complete the HST observations of the set of HST/Spitzer cross-calibration stars. Using a variety of standard stars with three different spectral types will ensure that the final calibration is not significantly affected by systematic uncertainties.
Execution	Two visits failed in this proposal but the observations were rescheduled and successfully executed. The two visits that failed were 07 (taken on September 16, 2010) and 11 (taken on September 15, 2010). The rescheduled visits were 57 (taken on April 26, 2011) and 61 (taken on April 28, 2011). Visits 07 and 11 consisted of both CCD and MAMA observations and the MAMA observations failed because of a decreed HV shutdown due to a lack of automatic shutdown failure during a safing incident. Visits 57 and 61 repeated the observations without any failures. All observations have been executed and accomplished in the time frame from November 6, 2009 to April 28, 2011.
Summary of Analysis	The bulk of the analysis will be in conjunction with a similar set of JWST flux standards observed in Cycle 18. The previously observed star GD71 is fully reduced and has been incorporated into the STIS WD flux calibration. P330E is also reduced and is currently under analysis for a STIS/ACS cross-calibration ISR. Most of the other stars have been observed by WFC3 for purposes of STIS/WFC3 cross-calibration.

Accuracy Achieved The ensemble absolute flux accuracy goal is 1% and may well be achieved after another year of hard work.

Continuation Plans This program has been continued into Cycle 18 as program 12428.

6. Supplemental Calibrations

Proposal ID 12078: Verification of Adjustment to Two STIS MSM Positions

Purpose and Description of Program

The STIS CCD mirror projects the center of the standard aperture onto the CCD detector near row 517, and the SIAF file assumes that all CCD spectroscopic gratings will project the target at this same location, apart from small differences of 1 - 2 pixels due to the non-repeatability of the MSM. In practice, the alignment of many of the CCD gratings deviates noticeably from this. Most of these offsets are sufficiently small that they have no operational consequences, but two settings deviate from the nominal position by an unusually large amount. The G430M 5216 centers the target near row 532, while the G750M 6094 is centered near row 490. When used with small sub-arrays, this can cause part of the target spectrum to fall outside the sub-array potentially ruining the science.

Execution

The single internal visit of 12078 was executed on April 19, 2010. Table 10, below, summarizes the exposures obtained. The observations using revised MSM values are marked with an "*". There were no anomalies or other problems with these observations.

Table 9. Mode Select Mechanism: Observations and SHIFT2A Values

Rootname	Optical Element	Central Wavelength	Aperture	Exposure Time	Lamp	SHIFT2A (Pixels)
ober01bpq	MIRVIS	N/A	52X0.1	1.0	Tungsten	N/A
ober01bqq	G430M	5093	52X0.1	10.0	HITM1	3.90
ober01brq*	G430M	5216	52X0.1	10.0	HITM1	5.70
ober01bsq	G430M	5471	52X0.1	10.0	HITM1	-2.27
ober01btq	G750M	5734	52X0.1	5.2	HITM1	3.82
ober01buq*	G750M	6094	52X0.1	4.2	HITM1	4.13
ober01bvq*	G750M	6094	0.2X0.2	4.2	HITM1	-0.96
ober01bxq	G750M	6252	52X0.1	4.1	HITM1	3.93

Summary of Analysis

Due to the structure of the MSM wheels, the translation between MSM cylinder wheel positions and the grating tilt is complex. Fortunately, two IDL routines, msm_cy_ea.pro, and msm_ea_cy.pro are available to translate between MSM cylinder positions and the grating tip and tilt angles. These routines are based on the c code program ALLMECT which was described in STIS SER TSW-011 (July 1994). The angles output by this code are defined such that changing the "elevation" angle moves the spectrum along the dispersion direction, while changing the "azimuth" angle moves it perpendicular to the dispersion.

The top panels in Figures 19 and 20 display the azimuthal angles for all CENWAVEs of the STIS G430M and G750M gratings. The diamond symbols show the original values, while the + mark in each upper panel shows the revised value that was being tested in this proposal. The lower panels show the SHIFTA2 values measured by CALSTIS from cross correlating the lamp spectrum with the nominal locations of the long-slit aperture bars using the STIS WAVECAL iraf task. The diamonds show results as measured using lamp spectra taken during the STIS calibration program 8916 in 2001, while the + signs mark the values measured during 12078 that tested the revisions for the 5216 and 6094 CENWAVE settings. Note that in addition to the revised setting being tested, wavecal spectra were also taken in each of the adjacent CENWAVE settings.

The 8916 data showed that the two settings with the most discrepant SHIFTA2 values also have discrepant azimuth settings. There was no apparent reason for these offsets; they appear to be errors in the original alignment calibration. So for these two settings the azimuth setting was revised to replace the old value with the interpolated value from the adjacent CENWAVE settings, and the new cylinder positions were calculated using the msm_ea_cy.pro routine. The STIS flight software tables were then revised to use these revised MSM cylinder positions for these CENWAVES by the software change request SCRS74 which was uplinked to HST on March 4, 2010 as part of the flight software build CS5.0/Ov006. Also see PR 64744 for additional details.

Summary of Analysis (cont.)

In the lower panels of Figures 19 and 20, the SHIFTA2 values measured during the execution of this program are shown by the + symbols. For the settings that were not revised, the agreement between the old and new offsets are within 2 pixels, which is about what would be expected given the limits on MSM repeatability and the typical thermal stability of the STIS bench. For the two revised settings the measured SHIFTA2 value is within the typical scatter of the other CENWAVE values.

For the G750M 6094 setting we included an extra wavecal exposure using the 0.2x0.2 aperture to simulate a point source spectrum. In the FLT file the spectrum is centered at row 516.07, which is within 1 pixel of where the flight software assumes the spectrum will be found. However, the SHIFTA1 value found by the CALSTIS wavecal task for this lamp spectrum using the 0.2x0.2 aperture differs by about 5 pixels from the shift found for the adjacent exposure that used the 52X0.1 aperture. Given that there was no MSM motion between the two exposures this is an unexpectedly large shift. If we compare the aperture bar locations measured in the G750M 6094 52X0.1 exposure with those in the MIRVIS lamp image, we find a shift of only 2/3 of pixel, well within the expected range MSM repeatability. This suggests that there may be a systematic offset in the tabulated positions for the aperture bars in a reference file.

Accuracy Achieved

For the G750M 6094 CENWAVE setting, the alignment in the cross dispersion direction now appears to be within 1 pixel of the alignment of adjacent CENWAVE settings. For the G430M 5216 setting, the previous SHIFTA2 offset of 19.7 pixels has been reduced to 5.7 pixels. This is larger than the median offset of about 3 pixels for this grating, but still smaller than 7.9 pixel offset of the G430M 3305 CENWAVE setting. Since the offset for the 5216 setting is now within the scatter seen for other settings, further adjustments are not recommended at this time.

Continuation Plans

This program was a one-time test of the revised MSM positions. Unless a decision was made to refine the other STIS MSM positions with smaller discrepancies, there is no need for a continuation program.

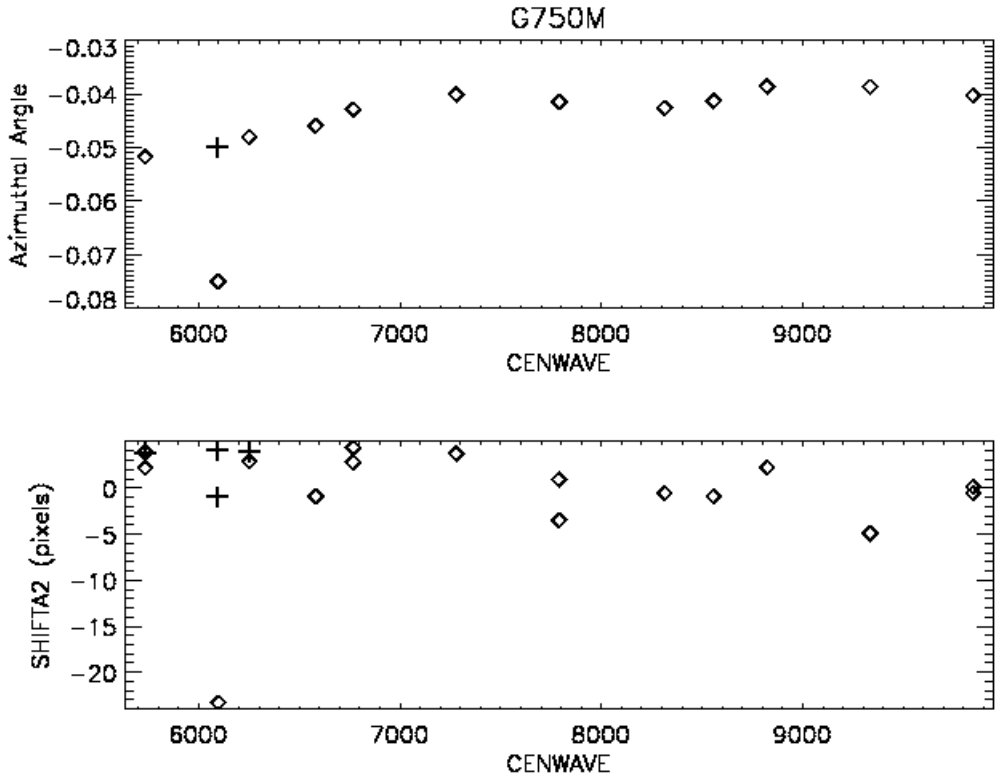

Figure 19. The top plot shows the azimuthal angle and the bottom plot presents the SHIFTA2 values as functions of central wavelength for G750M. In the upper panel, the diamond symbols show the original values, while the + mark shows the revised value that was being tested in this proposal. In the lower panel, the diamonds show results as measured using lamp spectra taken during the STIS calibration program 8916 in 2001, while the + signs mark the values measured during 12078.

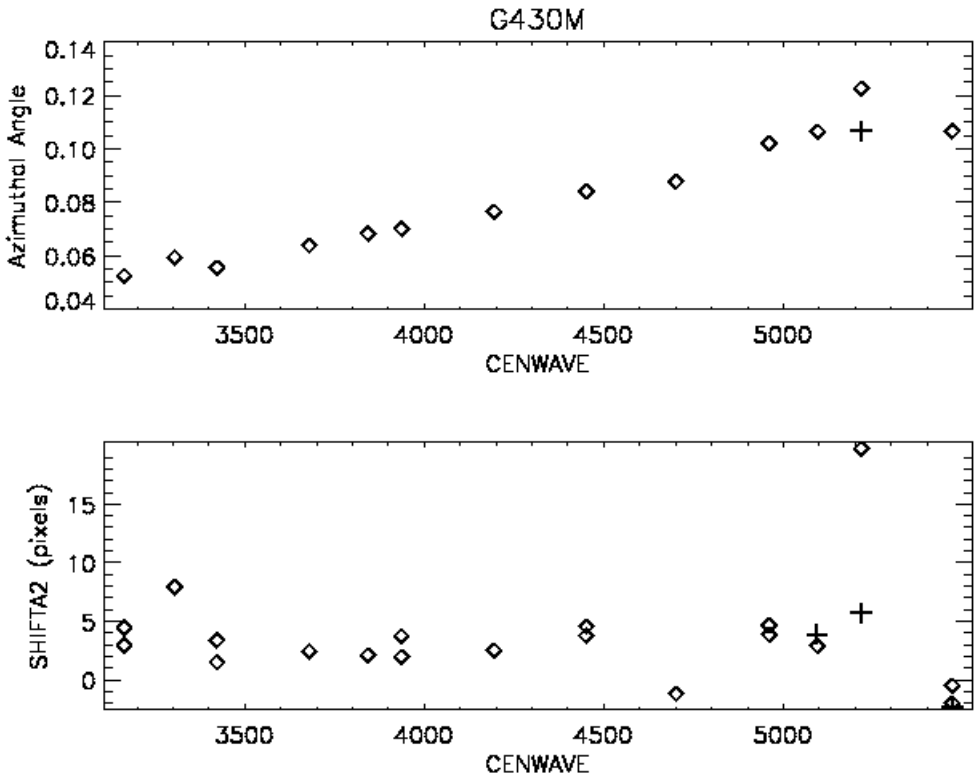

Figure 20. The top plot shows the azimuthal angle and the bottom plot presents the SHIFTA2 values as functions of central wavelength for G430M. Symbols are as in Figure 14.

Proposal ID 12079: STIS PtCr/Ne Lamp Ratios

Purpose and Description of Program	To get the full spectrum of the lamps brightness from the FUV to the optical wavelengths. Used 4 internal HST orbits to acquire lamp exposures with each of the LINE, HITM1, and HITM2 lamps.
Execution	There were no problems with the execution of the program.
Summary of Analysis	Analyzed both total counts within each grating as well as total counts within three narrower wavelength regions. Lamp ratios were then measured and compared to pre-launch ratios and to ratios from a similar calibration program taken early on in the STIS lifetime. This analysis confirms the fast decrease in the LINE lamp output at the shortest FUV wavelengths. There is an SPIE paper reporting these and other results related to the STIS and COS lamps (Pascucci et al. 2010), calibration workshop proceedings (Pascucci et al. 2010a), and an ISR (Pascucci et al. 2011).
Accuracy Achieved	It is found that the LINE lamp than that of the HITM lamps flux remains higher by about an order of magnitude at all wavelengths except at the shortest FUV wavelengths. At these short wavelengths, corresponding to the G140M-1173 setting, the HITM1 flux is currently 1.5 times higher than the LINE flux while the HITM2 flux is 3 times higher. The HITM2 flux is about 1.5 times higher than the HITM1 flux at all wavelengths. This fading is in the FUV faster than what expected from accelerated aging tests of the lamps in the laboratory. It is also shown that the COS lamps fade at the same rate as the STIS lamps.
Continuation Plans	There are no continuation plans for this program.

Change History for STIS ISR 2012-03

Version 1: May 8, 2013- Original Document

References

Bohlin, R. 1999, Instrument Science Report STIS 1999-06
Bostroem, K. A., et al., 2010, in Proc. 2010 HST Calibration Workshop, eds. S. Deustua & C. Oliveira, 456, http://www.stsci.edu/institute/conference/cal10/proceedings
Bostroem, K. A., et al. 2012, STIS Instrument Science Report 2012-01
Brown, T. M. & Davies, J. E., 2002 STIS Technical Instrument Report 2002-03
Dressel, L., et al., 2007, "STIS Data Handbook", Version 5.0
Goudfrooij, P., et al. 2006, PASP, 118, 1455
Niemi, S. M., 2010, STIS Technical Instrument Report 2010-01
Niemi, S. M., et al. 2010, in Proc. 2010 HST Calibration Workshop, eds. S. Deustua & C. Oliveira, 462, http://www.stsci.edu/institute/conference/cal10/proceedings
Pascucci, I., 2010, SPIE, 7731E, 105 and STIS Instrument Science Report 2010-01
Pascucci, I., et al., 2010a, in Proc. 2010 HST Calibration Workshop, eds. S. Deustua & C. Oliveira, 433, http://www.stsci.edu/institute/conference/cal10/proceedings
Pascucci I., et al. 2011, STIS Instrument Science Report 2011-01
Proffitt, C., et al., 2010, in Proc. 2010 HST Calibration Workshop, eds. S. Deustua & C. Oliveira, 41, http://www.stsci.edu/institute/conference/cal10/proceedings
Wolfe, M. A., et al., 2010, in Proc. 2010 HST Calibration Workshop, eds. S. Deustua & C. Oliveira, 443, http://www.stsci.edu/institute/conference/cal10/proceedings
Zheng, W., et al., 2010, in Proc. 2010 HST Calibration Workshop, eds. S. Deustua & C. Oliveira, 429, http://www.stsci.edu/institute/conference/cal10/proceedings
Zheng, W., et al. 2011, STIS Instrument Science Report 2011-03

7. Appendix

In this section the various types of publications written from Cycle 17 calibration data are presented. Table 10 provides information on the type and delivery date of reference files that have been updated and/or created with Cycle 17 calibration data. Table 11 lists instrument science reports and external publications produced as a result of analysis of Cycle 17 calibration programs. Table 12 presents all contributions made to the 2010 HST Calibration Workshop based on Cycle 17 calibration programs.

Table 10. STIS Cycle 17 Reference File Deliveries

Reference File	File Type	Delivery Date	Contributing Programs
CCD Reference Files			
CCD Bias	*bia.fits	October 28, 2010	11846, 11847
CCD Dark	*drk.fits	October 28, 2010	11844, 11845
CCD Flat Field	*pfl.fits	December 17, 2009	11852
CCD Parameters Table	*ccd.fits	September 10, 2009	11850
Time Dependent Sensitivity	*tds.fits	September 10, 2009	11855
FUV MAMA Reference Files			
FUV Time-Dependent Sensitivity	*tds.fits	July 12, 2010	11860
NUV MAMA Reference Files			
NUV Dark	*drk.fits	December 21, 2009	11857
NUV Dark Correction Table3	*tdc.fits	December 21, 2009	11857
NUV Photometric Conversion Table	*pht.fits	November 09, 2010	11860
NUV Time-Dependent Sensitivity	*tds.fits	November 09, 2010	11860
NUV Bad Pixel Table	*bpx.fits	February 14, 2010	11860

Table 11. Instrument Science Reports & Technical Instrument Reports Produced from Cycle 17 Calibration Programs

Number	Contributing Programs	First Author	Title
ISR2010-01 & 2010SPIE.7731E.105	12079, 11860	Pascucci, I.	Monitoring of the wavelength calibration lamps for the Hubble Space Telescope
ISR2011-01	11858, 11859	Pascucci, I.	Wavelength Calibration Accuracy for the STIS CCD and MAMA Modes
ISR2012-01	11866	Bostroem, K. A	Post-SM4 Sensitivity Calibration of the STIS Echelle Modes

Table 12. Contributions to the 2010 HST Calibration Workshop Based on STIS Cycle 17 Programs[1].

First Author	**Type**	**Title**
Bostroem, K. A.	Poster	Post - SM4 Flux Calibration of the STIS Echelle Modes
Niemi, S. M.	Poster	The Space Telescope Imaging Spectrograph Flat Fielding
Pascucci, I.	Poster	Monitoring of the Wavelength Calibration Lamps for the Hubble Space Telescope
Proffitt, C.	Talk	Performance of the Space Telescope Imaging Spectrograph after SM4
Wolfe, M. A.	Poster	Updated Status and Performance of the STIS CCD
Zheng, W.	Poster	Trend of Dark Rates of the COS and STIS NUV MAMA Detectors

[1] Proceedings of the calibration workshop can be found at:
http://www.stsci.edu./institute/conference/cal10/proceedings